TURUN
YLIOPISTO
UNIVERSITY
OF TURKU

METABOLIC EFFECTS OF THE GASTROINTESTINAL HORMONE SECRETIN
With focus on brown adipose tissue

Sanna Laurila

METABOLIC EFFECTS OF THE GASTROINTESTINAL HORMONE SECRETIN

With focus on brown adipose tissue

Sanna Laurila

University of Turku

Faculty of Medicine
Department of Internal Medicine
Doctoral programme in Clinical Research
Turku PET Centre

Supervised by

Professor Pirjo Nuutila, MD, PhD
Turku PET Centre, University of Turku
Turku, Finland

Docent Kirsi Virtanen, MD, PhD
Turku PET Centre, University of Turku
Turku, Finland

Reviewed by

Adjunct Professor
Kirsi Timonen, MD, PhD
Department of Clinical Physiology and
Nuclear Medicine, Central Finland
Health Care District, Jyväskylä, Finland

Docent, Chief Physician
Tiinamaija Tuomi, MD, PhD
Institute for Molecular Medicine Finland
Helsinki University Hospital and
University of Helsinki, Finland

Opponent

Professor Francesc Villarroya, PhD
Department of Biochemistry and
Molecular Biology,
University of Barcelona, Spain

Cover Image: Anna Skult (Figure 111. *Course and distribution of the Superior Mesenteric Artery* from the book by Triplett, William Harrison, *The Laws and Mechanics of Circulation, with the Principle Involved in Animal Movement*, 1885)

To my family and friends for their limitless support

UNIVERSITY OF TURKU
Faculty of Medicine
Internal Medicine
Turku PET Centre
SANNA LAURILA: Metabolic Effects of the Gastrointestinal Hormone
Secretin With Focus on Brown Adipose Tissue.
Doctoral Dissertation, 162 pp.
Doctoral Program in Clinical Research
August 2021

ABSTRACT

In recent years, brown adipose tissue (BAT) has been of interest in metabolic research, because its activity is associated with reduced cardiovascular risk, insulin resistance and obesity. Since cardiovascular disease accounts for the greatest cause of death globally, new treatments and methods of prevention are needed. BAT can burn fat instead of storing it, but it is likely that energy dissipation alone does not explain its health benefits. Meal induced BAT thermogenesis has recently been shown in humans, but its regulators and significance have never been pursued in detail. Since some gastric hormones have already shown both cardioprotective and appetite suppressing effects, they provide an interesting target for further studies.

Secretin is the oldest known hormone and belongs to a family of gastrointestinal peptides, secreted during feeding. The aim of this thesis was to study the metabolic effects of secretin beyond its well-known pancreatic exocrine stimulation. Mouse models were first implemented by collaborators at the Technical University of Munich to investigate the potential of using secretin to activate BAT thermogenesis and induce satiation. A placebo-controlled crossover study was then conducted at the Turku PET Centre with healthy male volunteers to study BAT activation, but also the broader pleiotropic effects of secretin. Tissue metabolic activity was quantified with positron emission tomography, using a fluoride labelled glucose tracer. Appetite was studied with functional magnetic resonance imaging.

Mouse models showed that secretin directly activates BAT thermogenesis through binding to the secretin receptor and that BAT thermogenesis in turn suppresses appetite. This novel satiation stimulating gut – BAT – brain axis was then shown in this thesis work to also translate to humans. Furthermore, myocardial glucose uptake was increased by secretin in humans. Previous studies have shown increased cardiac output by secretin and this thesis supports an inotropic effect. All in all, these results indicate that further clinical trials on secretin are warranted, as it could have potential applications in weight control and both preventing and treating heart disease.

KEYWORDS: gastrointestinal hormone, brown adipose tissue, positron emission tomography, appetite, metabolism, myocardial glucose uptake, functional magnetic resonance imaging, obesity, heart failure

TIIVISTELMÄ

Ruskea rasva on herättänyt kiinnostusta viime vuosina, koska sen aktiivisuuden on osoitettu olevan yhteydessä insuliiniherkkyyteen, normaaliin painoon ja pienentyneeseen sydän- ja verisuonitauti riskiin. Näistä viimeinen on suurin kuolinsyy maailmanlaajuisesti. Ruskea rasva polttaa rasvaa sen varastoimisen sijaan, mutta todennäköisesti sen terveysedut eivät johdu ainoastaan lisääntyneestä energiankulutuksesta. Ruokailu aktivoi ruskeaa rasvaa, mutta ilmiön säätelyä ja merkitystä ei ole aiemmin selvitetty tarkasti. Ruoansulatushormonit muodostavat mielenkiintoisen tutkimuskohteen ruskean rasvan aktivoimisen suhteen, koska osalla niistä tiedetään olevan sydäntä suojaavia ja ruokahalua vähentäviä vaikutuksia.

Sekretiini on vanhin tunnettu hormoni. Sitä erittyy verenkiertoon ruokaillessa ja se aktivoi haiman eksokriinistä eritystä. Tässä väitöskirjassa tutkittiin sekretiinin muita mahdollisia aineenvaihdunnallisia vaikutuksia. Sen vaikutus ruskean rasvan aktivaatioon ja ruokahaluun selvitettiin ensin hiirimalleilla Münchenin teknillisessä yliopistossa, jonka jälkeen Turun PET-keskuksessa toteutettiin lumekontrolloitu, tapaus-ristikkäistutkimus terveillä miehillä. Kudosten aineenvaihduntaa tutkittiin fluorileimatulla glukoosimerkkiaineella ja positroniemissiotomografialla. Ruokahalua tutkittiin funktionaalisella magneettikuvantamisella.

Hiirimallilla osoitettiin, että sekretiini aktivoi suoraan ruskean rasvan lämmöntuotantoa sitoutumalla sekretiinireseptoriin, mikä puolestaan johti ruokahalun vähenemiseen. Tämä uusi ruokahalua säätelevä mekanismi osoitettiin myös ihmisillä. Sen lisäksi sekretiini lisäsi ihmisillä sydämen glukoosin soluunottoa. Aikaisemmissa tutkimuksissa on osoitettu, että sekretiini lisää sydämen minuuttitilavuutta, joten väitöstyö vahvistaa, että sekretiinillä on inotrooppinen vaikutus. Tulokset osoittavat, että sekretiiniä tulisi tutkia kliinisesti laajemmin, sillä se voisi auttaa painonhallinnassa, sekä estää ja hoitaa sydänsairauksia.

AVAINSANAT: ruoansulatushormoni, ruskea rasva, positroniemissiotomografia, ruokahalu, aineenvaihdunta, sydämen glukoosin soluunotto, funktionaalinen magneettikuvantaminen, lihavuus, sydämen vajaatoiminta

Table of Contents

Abbreviations

AgRP	Agouti-related protein
ANS	Autonomic Nervous System
ATP	Adenosine triphosphate
AUC	Area under the curve
β-AR	Beta adrenergic receptor
BAT	Brown adipose tissue
BMI	Body mass index
BOLD	Blood-oxygen-level-dependent
BPM	Beats per minute
cAMP	Cyclic adenosine monophosphate
CCK	Cholecystokinin
CCS	Composite satiety score
CT	Computer tomography
DOPA	Dihydroxyphenylalanine
ECG	Electrocardiography
ECLIA	Electrochemiluminescence immunoassay
EE	Energy expenditure
ELISA	Enzyme-linked immunosorbent assay
EPI	Echo-planar imaging
FA	Fatty Acid
FDR	False discovery rate
[^{18}F]FDG	[^{18}F]2-fluoro-2-deoxy-D-glucose
fMRI	Functional magnetic resonance imaging
FOV	Field of view
FUR	Fractional uptake rate
GABA	Gamma-aminobutyric acid
GHRH	Growth hormone-releasing hormone
GIP	Gastric inhibitory peptide
GLP-1	Glucagonlike peptide-1
GU	Glucose uptake
H+	Hydrogen proton

HU	Hounsfield Unit
iBAT	Intrascapular BAT
ISO	Isoproterenol
K_i	Net uptake rate
KO	Knock-out
LC	Lumped constant
MRI	Magnetic resonance imaging
MSOT	Multispectral optoacoustic tomography
NMR	Nuclear magnetic resonance
OCR	Oxygen consumption rate
PACAP	Pituitary adenylate cyclase-activating polypeptide
PET	Positron emission tomography
PKA	Protein kinase A
POMC	proopiomelanocortin
QTc	Heart rate corrected QT interval
ROI	Region of interest
RPKM	Reads per kilobase per million mapped reads
SCTR	Secretin receptor (human)
Sctr	Secretin receptor (murine)
SD	Standard deviation
SGLT2	sodium-glucose transporter protein 2
SNS	Sympathetic nervous system
SUV	Standard uptake value
TAC	Time activity curve
TG	Triglyceride
TRPV1	Transient receptor potential vanilloid 1
UCP1	Uncoupling protein 1
VAS	Visual analogue scale
VIP	Vasoactive intestinal peptide
WAT	White adipose tissue
WT	Wild type

List of Original Publications

This dissertation is based on the following original publications, which are referred to in the text by their Roman numerals:

I   Li Y.*, Schnabl K.*, Gabler S.M., Willershäuser M., Reber J., Karlas A., Laurila S., Lahesmaa M., U-Din M., Bast-Habersbrunner A., Virtanen K.A., Fromme T., Bolze F., O'Farrell L.S., Alsina-Fernandez J., Coskun T., Ntziachristos V., Nuutila P., Klingenspor M. Secretin-Activated Brown Fat Mediates Prandial Thermogenesis to Induce Satiation. *Cell*, 2018; 175(6):1561-1574.e12; doi: 10.1016/j.cell.2018.10.016.

II   Laurila S., Sun L.*, Lahesmaa M.*, Schnabl K., Laitinen K., Klén R., Li Y., Balaz M., Wolfrum C., Steiger K., Niemi T., Taittonen M., U-Din M., Välikangas T., Elo L.L., Eskola O., Kirjavainen A., Nummenmaa L., Virtanen K.A., Klingenspor M., Nuutila P. Secretin Activates Brown Fat and Induces Satiation in Humans. *Nature Metabolism*, 2021; 3:798-809; doi: 10.1038/s42255-021-00409-4.

III Laurila S., Rebelos E. Lahesmaa M., Sun L., Schnabl K., Peltomaa T-M., Klén R., U-Din M., Honka M., Eskola O., Kirjavainen A., Nummenmaa L., Klingenspor M., Virtanen K.A., Nuutila P. Novel Effects of the Gastrointestinal Hormone Secretin on Myocardial Metabolism and Renal Function. **Manuscript.**

The original publications have been reproduced with the permission of the copyright holders.

1   Introduction

The concept of endocrine regulation was introduced in 1902 by Bayliss and Starling, when they discovered that an active agent, produced by the gut, stimulates pancreatic secretion, independent of the vagus nerve (Bayliss and Starling, 1902). They named the hormone "secretin". Later, it has been discovered that secretin receptors are not only present in the pancreas, but in nearly every organ throughout the body (Afroze et al., 2013). Secretin's close sibling glucagonlike peptide-1 (GLP-1) has proven to have great clinical significance. GLP-1 agonists are not only effective glucose lowering medicines in type two diabetes, but also aid weight loss in obesity (Astrup et al., 2009). GLP-1 has also piqued an interest in the field of cardiology due to its agonists showing benefits on cardiac mortality (Cosentino et al., 2020). Despite the recent re-emergence of interest in gastric peptides, there have been very few studies on secretin. Modern imaging methods provide a unique opportunity to investigate organ crosstalk *in vivo*, and the broad effects that the oldest known hormone may have.

There is evidence from 40 years past, that secretin increases cardiac output and stroke volume in heart failure patients (Gunnes and Rasmussen, 1986). An inotropic effect was suggested, but this could not be proven with the implemented method. At the time, the potential of secretin as a heart failure medication was not further pursued, likely due to the challenges of intravenous administration and its short half-life, as well as concomitant breakthroughs in heart failure treatment (CONSESUS, 1987). Despite therapeutic advances, cardiovascular diseases are still the leading cause of death world-wide and both new treatment and prevention options are needed (Roth et al., 2018).

Another more recently confirmed pleiotropic effect of secretin is that the hormone induces lipolysis in white adipose tissue (WAT) (Sekar and Chow, 2014). Interestingly, lipolysis is important in the initiation of thermogenesis in brown adipose tissue (BAT), but the hormone's effect on BAT has so far not been pursued (Braun et al., 2018). BAT is known for cold induced non-shivering thermogenesis and its activity has recently been linked to reduced cardiovascular risk in humans (Becher et al., 2021). Meal induced BAT thermogenesis has been recognized in rodents decades ago (Glick et al., 1981; Rothwell and Stock, 1979) and recently also

in humans (U-Din et al., 2018). It has been speculated that the phenomenon is induced by sympathetic activation, but results have been conflicting (Cannon and Nedergaard, 2004). A hormonal pathway is possible, but this has not been thoroughly investigated.

The significance of meal induced BAT activation has been debated, but appetite suppression has been proposed (Chondronikola et al., 2017; Crovetti et al., 1998). So far, this hypothesis has never been thoroughly tested in mice or humans. Humans have a relatively small BAT mass compared to mice, so there may be regulatory effects that are beneficial to cardiometabolic health, instead of BAT simply increasing catabolism (Villarroya et al., 2016). Obesity increases the risk of type two diabetes and cardiovascular disease and is increasing worldwide (Bessesen and Van Gaal, 2018). If confirmed, thermogenic appetite regulation could offer new possibilities for treatment and prevention of obesity. Incidentally, secretin has been shown to have an appetite suppressing effect in mice (Chen et al., 2011), but its effect on appetite in humans is not known. If secretin has a beneficial effect on both appetite and cardiac function, it could have potential in both treating and preventing heart disease.

2 Review of the Literature

2.1 Secretin, the first hormone discovered

In the late 19th century, Pavlov showed that pancreatic secretion is controlled by two mechanisms: the vagus nerve and acidic content of the stomach coming in contact with the duodenal mucosa (Babkin, 1949). However, according to him, both mechanisms were conveyed through the nervous system. In 1902, Bayliss and Starling proved the existence of a new mechanism altogether (Bayliss and Starling, 1902). They infused 0.4% hydrochloric acid into a jejunal loop that had been denervated and showed that this produced secretion by the pancreas for a few minutes. Their conclusion was that the jejunal mucosa produces an active chemical messenger, carried by blood from a producing organ to another; a "hormone" called "secretin".

It took decades, before the existence of secretin was confirmed. Porcine secretin was purified in the 1960s (Jorpes and Mutt, 1961) and soon after, its amino acid sequence was determined (Mutt et al., 1970). Soon, secretin was also chemically synthesized (Bodanszky et al., 1967). Its hormonal action was finally proven in 1970, when elevated plasma secretin levels were shown in dogs and humans, both by duodenal acidification and the ingestion of a meal (Chey et al., 1978; Kim et al., 1979; Schaffalitzky De Muckadell and Fahrenkrug, 1978). Later the effect of the hormone was further proven, when it was shown that an intravenous infusion of secretin induces pancreatic fluid and bicarbonate secretion (Chey et al., 1979). The last piece of the hypothesis introduced by Bayliss and Starling was proven in 1981, when Gardner et al. showed the existence of secretin receptors (sctr) in the pancreas (Gardner and Jensen, 1981).

Secretin consists of 27 amino acid residues and the sequence is highly similar between different animal species (Chey and Chang, 2014). It belongs to a peptide superfamily of gastrointestinal hormones, which are shown in **Table 1**. Secretin binds to SCTR, which is a G protein-coupled receptor that activates cyclic adenosine monophosphate (cAMP) signalling (Dong and Miller, 2002). Although it is best known for its gastrointestinal function, SCTR are found in most organs and tissues, indicating that secretin is a pleiotropic hormone with a multitude of functions.

Currently synthetic secretin is in clinical use for rare and specific diagnostic purposes. In Zollinger-Ellison Syndrome, a rare neuroendocrine tumour (gastrinoma) produces high levels of gastrin (Metz, 2012), which leads to abnormally increased gastric acid output. When a gastrinoma is suspected but serum gastrin levels and gastric pH is undiagnostic, a secretin test can be performed. Secretin stimulates gastrinoma cells to release gastrin, which leads to a pronounced increase in serum gastrin levels. Secretin is also sometimes used for diagnosing exocrine pancreatic insufficiency (Dreiling, 1975; Moolsintong and Burton, 2008). In some centres, it is used during magnetic resonance cholangiopancreatography, in order to evaluate the anatomy of the pancreatic duct and pancreatic exocrine function (Chamokova et al., 2018).

Table 1. Intestinal polypeptide superfamily in humans. Modified from Chey and Chang 2003.

Peptide	Discovered or isolated by
Secretin	Bayliss and Starling 1902
Glucagon	Kimball and Murlin 1923
Gastric inhibitory peptide (GIP)	Brown et al. 1970
Vasoactive intestinal peptide (VIP)	Said and Mutt 1974
Glicentin (proglucagon)	Moody et al. 1976
Oxyntomodulin (glucagon-37)	Bataille et al 1981
Peptide PHI	Tatemoto and Mutt (1981)
Glucagon-like peptide -1 and -2 (GLP-1 and-2)	Lund et al 1982
Growth hormone-releasing hormone (GHRH)	Guillemin et al 1982
Pituitary adenylate cyclase-activating polypeptide (PACAP)	Miyata et al. 1989
Orexin	De Lecea el al 1998 (Sakurai et al 1998)

2.1.1 Secretin as a gastrointestinal hormone

Secretin is predominantly synthesized by the S-cells in the crypts of Lieberkühn of the duodenum (Häcki, 1980). During feeding, the acidic contents of the stomach move into the duodenum, which prompts the release of secretin into the circulation (Häcki, 1980). This is mediated by the secretin releasing peptide in the upper small intestinal lumen (Li et al., 1990). Secretin, along with VIP, cholecystokinin (CCK) and vagal stimulation, increases pancreatic exocrine secretion (Afroze et al., 2013). Secretin also stimulates pancreatic acinar cells to produce bicarbonate and water, and inhibits gastric acid secretion and gastric motility (Afroze et al., 2013). The intestinal lining is protected by the neutralization of its acidic contents and digestive enzymes

start to break down nutrients (Afroze et al., 2013). Pancreatic proteases also break the secretin releasing peptide, creating a negative feedback loop (Li et al., 1990). In addition to influencing the pancreas, secretin also induces biliary secretion of water, bicarbonate and chloride (Chey and Chang, 2014), but not bile acids (Pissidis et al., 1969).

2.1.2   Secretin as a neuropeptide

In addition to the well-established exocrine effects on the pancreas, secretin has a multitude of other functions. It was first recognized as a possible neuropeptide in 1979, when secretin-like bioactivity was found in porcine brain extracts (Mutt et al., 1979). Since then, secretin peptide expression has been plotted in several different brain regions, mostly in rodent models (**Figure 1.**) (Wang et al., 2019). One study on human brains found secretin immunoreactivity in cerebellar Purkinje cells, deep cerebellar nuclei, pyramidal neurons of the motor cortex and, in addition to findings in rodents, also the hippocampal and amygdala nuclei (Köves et al., 2004). Spatially, the secretin receptor is even more widely distributed than its ligand, which may indicate that several different neuronal functions could be modulated by secretin (Ng et al., 2002). Secretin may also be important in early postnatal, hippocampal neurogenesis; in mice, its deficiency leads to impaired neurobehavioral development (Jukkola et al., 2011). In secretin deficient mice, there was impaired synaptic plasticity in the hippocampus (Yamagata et al., 2008).
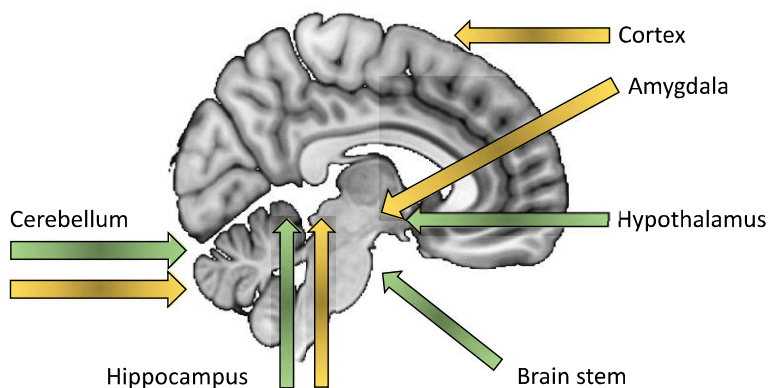

Figure 1.   Central secretin peptide and receptor distribution according to animal studies is marked with green arrows. Presence of secretin peptide by immunohistochemistry in human studies is marked with yellow arrows. Modified from Wang et al. 2019.

Secretin has been shown to have regulatory effects on catecholamine metabolism in the axon terminals of sympathetic nerves (Schwarzschild and Zigmond, 1989). It has a stimulatory effect on cAMP production (Propst et al., 1979), which regulates the enzyme tyrosine hydroxylase (Ip et al., 1985). This enzyme catalyzes the rate limiting step of catecholamine biosynthesis and secretin has been shown to increase tyrosine hydroxylase activity in the sympathetic ganglia and several autonomic end organs (Schwarzschild and Zigmond, 1991). In the central nervous system, this same increase in tyrosine hydroxylase activity has been shown in the hypothalamus with an interventricular infusion of secretin in rats (Babu and Vijayan, 1983).

Rodent studies indicate that secretin is involved in the regulation of dihydroxyphenylalanine (DOPA) synthesis and turnover (Chu et al., 2006). Secretin also facilitates gamma-aminobutyric acid, or GABAergic input of Purkinje cells in the cerebellum (Lee et al., 2005; WH et al., 2001) and vasopressin expression and release in the hypothalamus (Chu et al., 2006). However, this effect on both vasopressin and oxytocin release may also be through a noradrenergic pathway, as shown in a rat model by Velmurugan et al (Velmurugan et al., 2010). All in all, it has been proposed, that the central actions of secretin are related to fluid homeostasis (Chu et al., 2009, 2011), food intake (Butcher and Carlson, 1970) and control of social behavior (Horvath et al., 1998; Sandler et al., 1999). These effects by peripherally secreted secretin would be mediated through the autonomic nervous system (ANS) (Chu et al., 2013; Yang et al., 2004), or directly after transmembrane diffusion of the hormone (Banks et al., 2002).

2.1.2.1   Social behaviour

Twenty years ago, secretin gained attention as a possible target for the treatment of autism, when Horvath and colleagues reported improved social, cognitive and communicative skills in three autistic children, who had received intravenous injections of synthetic secretin during endoscopic evaluations of gastric problems (Horvath et al., 1998). There is a loss of cerebellar Purkinje cells in autism (Bauman, 1991) and as mentioned previously, secretin is known to facilitate the function of these cells (Lee et al., 2005; WH et al., 2001). Genes encoding oxytocin and vasopressin have also been suggested as candidates for autism and social phobias (Young, 2001) and secretin has an effect on them as well (Velmurugan et al., 2010). Despite interest and several randomized, placebo-controlled clinical studies, intravenous secretin showed no statistically significant benefit in language, cognition or autistic symptoms, compared to placebo (Krishnaswami, 2011; Sandler et al., 1999).

2.1.2.2 Appetite

Secretin's role in the control of food intake was postulated in mice already in the 1970's (Butcher and Carlson, 1970). Later, the anorexigenic effect of secretin was suggested to depend on melanocortin signaling, shown with both peripheral and central administration of the hormone in mice (Chen et al., 2011). The same group later showed that vagotomy and capsaicin, an afferent neurotoxic treatment, attenuated the anorexigenic effects of peripherally administered secretin (Chu et al., 2013).

Several other gastric hormones have been shown to have effects on appetite. Those with well-established anorexigenic effects, together with the adipokine leptin, are CCK, pancreatic polypeptide, peptide YY, GLP-1 and oxyntomodulin, while the only known orexigenic hormone is ghrelin (Paz-Filho et al., 2015; Perry and Wang, 2012). So far, there have been no studies addressing the anorexigenic effects of secretin in humans.

2.1.2.3 Fluid homeostasis

Initially it seemed that secretin had a diuretic effect on dogs and humans (Barbezat et al., 1972; Owen and Ivy, 1931), however there were opposite findings in rats (Charlton et al., 1986). Secretin increases renal blood flow in rats (Lameire et al., 1980), and single-nephron glomerular filtration rate and glomerular plasma flow in dogs (Marchand, 1986). More recently it was shown in mice, that secretin is released from the posterior pituitary during hyperosmolar conditions and that it stimulates vasopressin expression and release in the hypothalamus (Chu et al., 2009). In a study that utilized secretin receptor null mice, it was shown that secretin has a vasopressin -independent mechanism on aquaporin 2 channels in the collecting tubules, increasing renal water absorption (Chu et al., 2007). Centrally injected secretin induced water drinking behavior and thus also increased diuresis in rats, while peripherally injected secretin did not have this effect (Chu et al., 2011). Results are thus somewhat conflicting, and it may be that secretin has opposite effects on fluid homeostasis, depending on whether the effect is central or peripheral, or relating to conditions such as osmolarity or serum secretin concentration.

2.1.3 Secretin's cardiovascular effects

Recently, there has been great interest in the cardiac effects of gastric peptides, due to GLP-1 agonists showing cardiac benefits in diabetic patients (Cosentino et al., 2020). Secretin's cardiac effects were investigated long before the recent interest and then forgotten. In the 80's, a combined inotropic and vasodilating effect was suggested in humans. Secretin was shown to increase cardiac output and stroke

volume in heart failure patients (Gunnes and Rasmussen, 1986). In patients with angina, who had normal ventricular function, systemic resistance decreased, stroke volume increased and mean cardiac output increased with 20 percent (Gunnes et al., 1983). There is also indirect evidence of secretin having an association with normal cardiac function, as secretin and gastrin-releasing peptide were significantly lower in patients with chronic heart failure, compared to controls (Nicholls et al., 1992). This was not the case with VIP, GIP, insulin, or glucagon.

The cardiac effects of secretin have been studied in few animal models. In rat cardiomyocytes, the presence of nonselective VIP and secretin receptors, as well as secretin-preferring receptors, has been shown (Bell and McDermott, 1994). Secretin stimulated contraction, due to accumulation of cAMP in cells (Bell and McDermott, 1994). In pigs, intracoronary secretin increased cardiac function and perfusion through nitrogen monoxide release and β-adrenoceptors (Grossini et al., 2013). In coronary endothelial cells, this was caused through cAMP signaling (Grossini et al., 2013). The effects were abolished by a secretin receptor agonist (Grossini et al., 2013). All these effects are G_s-protein coupled, but G_q-coupling of sctr is also recognized (Garcia et al., 2012). Instead of cAMP signaling, G_q-coupled activation mobilizes intracellular calcium (Garcia et al., 2012). This could also contribute to increased cardiomyocyte contraction, but the effect has not been investigated.

2.1.4   Secretin's effects on lipid and glucose metabolism

Secretin activates lipolysis in WAT (Butcher and Carlson, 1970; Sekar and Chow, 2014). It binds to sctr, which activate cAMP-protein kinase A (PKA) signaling in murine white adipocytes, independent of sympathetic activation (Braun et al., 2018). During prolonged fasting, plasma secretin levels are increased almost 8-fold from day 1 to 3 (Bell et al., 1985; Clark Mason et al., 1979; Manabe et al., 1987). This level is much higher than the levels achieved through intraduodenal acidification and is most likely due to secretin being a potent lipolytic agent (Butcher and Carlson, 1970; Sekar and Chow, 2014).

It has also been shown that secretin acts as an incretin during glucose stimulation (Lerner and Porte, 1972). Insulin secretion was increased by secretin during a glucose infusion and pretreating patients with secretin also potentiated glucose stimulated insulin release (Lerner and Porte, 1972). The small increase in insulin levels in individuals who fasted only lasted a few minutes and authors suggested that secretin only stimulates the first phase of insulin release, not production (Lerner and Porte, 1970).

2.2 Brown adipose tissue

BAT has been of interest in the field of obesity and metabolic research ever since it was established in 2009 by three different groups, that adult humans have metabolically active BAT (Cypess et al., 2009; van Marken Lichtenbelt et al., 2009; Virtanen et al., 2009). Instead of storing triglycerides (TG) like WAT, BAT is also able to utilize the stored energy with mitochondrial uncoupling protein 1 (UCP1) to produce heat. This thermogenic effect is known to be important for thermal regulation in small rodents (Jakus et al., 2008), but also in humans during infancy (Aherne and Hull, 1966).

In adult humans, the catabolic potential of BAT has been of interest in obesity research. It has been calculated, that supraclavicular BAT could burn up to four kilograms of fat yearly, if constantly activated (Virtanen et al., 2009). In humans, cold activation of BAT has been shown to negatively associate with age and body mass index (BMI) (Cypess et al., 2009; Saito et al., 2009). BAT activation is also associated with insulin sensitivity (Chondronikola et al., 2014; Hanssen et al., 2015), lowered circulating TGs (U-Din et al., 2017) and cardiovascular health (Becher et al., 2021). Obese persons have less cold induced BAT activation, but weight loss with exercise and nutritional guidance, or with gastric bypass surgery, increases BAT mass (Orava et al., 2013; Vijgen et al., 2012). Since BAT's catabolic potential in humans is somewhat blunted by its relatively small mass, it has been proposed that BAT may also have beneficial regulatory effects (Ikeda et al., 2018). These effects may be conveyed by afferent neuronal communication with the brain, as well as through secretion of adipokines and lipokines (Villarroya et al., 2017). For instance: BAT activation counteracts insulin resistance by suppressing WAT fibrosis through lipokines (Ikeda et al., 2018).

2.2.1 Structure and location

BAT is densely innervated and vascularized (Cannon and Nedergaard, 2004). The lipid droplets in BAT are small compared to WAT and brown adipose cells have an abundance of mitochondria (**Figure 2**). In addition to classic BAT, literature also mentions beige or brite adipose tissue, which in mice is histologically closer to adult human BAT. Currently beige adipose tissue is considered to be the same plastic tissue as BAT, which adapts to its prevalent environment by varying its expression of UCP1 (Kalinovich et al., 2017). When UCP1 expression is downregulated, this adipose tissue turns white-like and when it is upregulated, it turns brown-like.
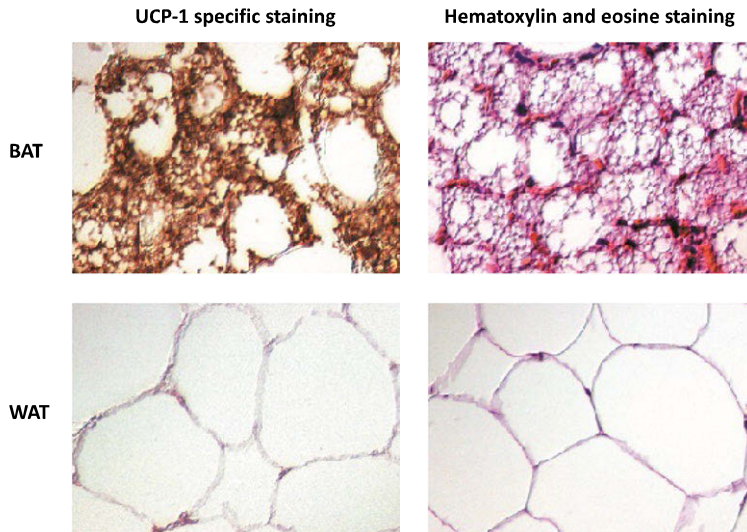
Figure 2. Microscopic image of BAT and WAT. Modified from Virtanen et al. 2009.

BAT is formed during human fetal development and infants have an abundance of BAT around the shoulder blades (Aherne and Hull, 1966; Ponrartana et al., 2013). During childhood, the amount of BAT is reduced until it increases again in puberty, as muscle mass increases (Ponrartana et al., 2013; Rogers, 2015). In adulthood, relative BAT mass decreases with age. The largest BAT depots in humans are located in the neck and above the clavicles, but according to autopsy data, smaller BAT depots are located throughout the body, especially around vital organs (Heaton, 1972) (**Figure 3.**). Human BAT function can be studied with positron emission tomography (PET) combined with computed tomography (CT) -imaging. Current estimates on BAT mass have been made by studying these largest depots only and thus likely underestimate the catabolic capacity of human BAT (Kim et al., 2019).
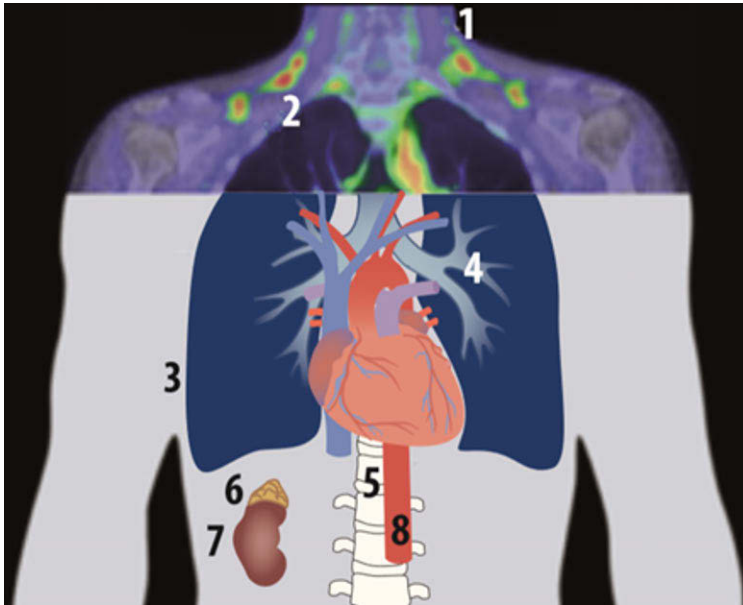
Figure 3. The top image shows a PET/CT image of the neck area, where the glucose uptake of 1. cervical and 2. supraclavicular BAT can be quantified. The lower image shows the known anatomical locations of BAT, which cannot be quantified with current PET/CT technology: 3. axilla, 4. lung hilum and pericardial fat pad, 5. aortic, 6. adrenal, 7. renal and 8. paravertebral. Modified from Laurila et al. 2020.

2.2.2   Cold induced brown adipose tissue activation

The strongest known activator of BAT thermogenesis is cold exposure, which also increases UCP1 expression (Blondin et al., 2014; van der Lans et al., 2013; Yoneshiro et al., 2013). This is why BAT is more active in a colder climate, even in humans (Cypess et al., 2009; Huttunen et al., 1981; Saito et al., 2009).

Brown adipose tissue is activated by exposure to cold through the sympathetic nervous system (Cannon and Nedergaard, 2004). Thermal receptors on the skin sense temperature and relay the signal to the brain. Efferent sympathetic nerves then bring the signal to BAT (**Figure 4.**). Noradrenaline and adenosine triphosphate (ATP), which breaks into adenosine, are released from the sympathetic nerve endings (Kooijman et al., 2015; Lahesmaa et al., 2019). Noradrenaline binds to $\beta 3$-adrenoceptors and adenosine to A_{2A}-receptors, which leads to intracellular lipolysis and UCP1 activation. Fatty acids (FA) are released from TGs, stored in intracellular lipid droplets. At the same time, an influx of FA and glucose into the cell is initiated, to restore these TG storages.

Released FAs are taken into the mitochondrial matrix, where they fuel the Krebs cycle (**Figure 4**). Hydrogen protons (H^+), created in the Krebs cycle, are transported through the electron transport chain into the intermembrane space. A proton gradient

is formed between the mitochondrial matrix and the intermembrane space, which is mostly utilized in the production of ATP. In BAT, however, this proton gradient is uncoupled from ATP synthase by UCP1, and energy is instead released as heat.
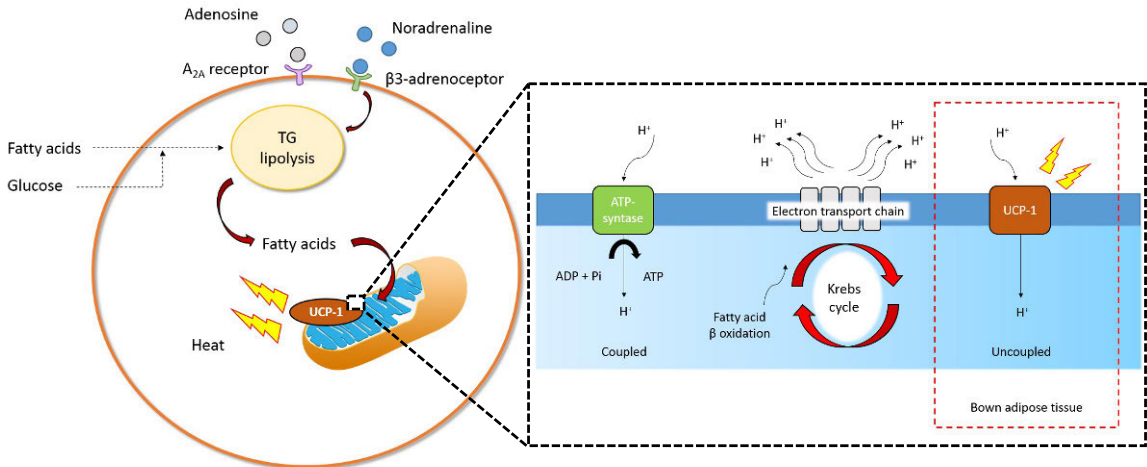

Figure 4. UCP1 induced thermogenesis in brown adipose cells. Modified from Laurila et al. 2020.

2.2.3 Meal induced brown adipose tissue activation

Meal induced thermogenesis consists of handling thermogenesis, produced through ingestion, digestion and absorption, and facultative thermogenesis, the latter which has sometimes been disputed (Kozak, 2010). Regardless, meal induced BAT thermogenesis has been known in rodents for decades (Glick et al., 1981; Rothwell and Stock, 1979). Although meal induced thermogenesis has been recognized in humans, it was long unclear whether BAT contributes to it.

Postprandial BAT thermogenesis was proven in humans recently, when BAT oxygen consumption was shown to significantly increase after a mixed meal, to the same level as during cold exposure (U-Din et al., 2018). Before this, it was shown that a high calorie, carbohydrate rich meal increases BAT activity, measured semi quantitatively with [^{18}F]2-fluoro-2-deoxy-D-glucose ([^{18}F]FDG) PET/CT, in lean humans (Vosselman et al., 2013). BAT is insulin sensitive (Orava et al., 2011) and the increase was associated with insulin levels. Vrieze et al. showed the opposite with the same imaging method after a mixed meal; BAT standard uptake was decreased compared to a fasting state (Vrieze et al., 2012). This could have been due to the semi quantitative method used and the relatively higher uptake in muscles affecting the result, but the authors also speculated that BAT may utilize fatty acids instead of glucose after a mixed meal. This increase in fatty acid uptake after a mixed

meal compared to fasting conditions was later confirmed by U-Din et al. (U-Din et al., 2018).

Postprandial thermogenesis, including that produced by BAT, has been assumed to be mediated through the sympathetic nervous system (SNS). During feeding, circulating glucose and insulin levels are increased and sensed by the hypothalamus, which in turn increases sympathetic drive (Cannon and Nedergaard, 2004). However, only carbohydrates activate the SNS, yet thermogenesis is induced by all macronutrients (Welle et al., 1981). It has thus also been suggested that dietary peptides, released during feeding, are sensed by the brain, which then activates thermogenesis through the SNS (Bachman et al., 2002). This was shown with a central administration of GLP-1 in mice (Beiroa et al., 2014), whereas in the case of CCK, it was proposed that sympathetic afferents deliver the message to the central nervous system (Blouet and Schwartz, 2012). However, nonselective β-blockade does not reduce postprandial metabolic rate (Thörne and Wahren, 1989; Zwillich et al., 1981), which indicates that thermogenesis is initiated by a mechanism independent of the SNS. Interestingly, the bile acid chenodeoxycholic acid increases BAT thermogenesis through an SNS independent pathway (Broeders et al., 2015). Bile acids are ejected into the intestine during feeding, after which 95 percent are reabsorbed and enter the portal blood stream (Yang and Zhang, 2020). They could therefore also facilitate postprandial BAT activation.

In 1979, Rothwell and Stock proposed that the purpose of prandial BAT thermogenesis is to burn off excess calories and protect against obesity and insulin resistance (Rothwell and Stock, 1979). They discovered that rats that were fed high calorie diets, gained less weight than was expected from their caloric intake. Recently a creatin-driven substrate cycle in beige adipose tissue was shown to have a role in diet induced thermogenesis in mice (Kazak et al., 2017). When adipose creatin metabolism was genetically depleted, diet induced obesity occurred without an increase in caloric intake, compared to non-genetically depleted mice (Kazak et al., 2017). From an evolutionary standpoint however, the concept might seem counterintuitive, since high calorie conditions are extremely rare and in essence only persist in modern human societies (Kozak, 2010). The idea of an impaired metabolic rate causing obesity lead to years of search for obese patients with low metabolism, but such patients were never found (Prentice and Jebb, 2004). Besides, there is a well proven positive association between body weight and resting metabolic rate (Leibel et al., 1995).

BAT thermogenesis has also been suggested as a regulator of food intake (Glick, 1982; Himms-Hagen, 1995). In humans, there is indirect evidence for the role of thermogenesis on appetite. A thermogenic meal is associated with a sensation of fullness (Crovetti et al., 1998) and BAT activation, induced by mild cooling, lowers circulating ghrelin levels (Chondronikola et al., 2017). However, thermoregulatory

feeding has not been extensively studied, possibly because it was known that nonselective β-blockade does not increase meal sizes and UCP1 knock-out (KO) mice do not feed excessively (Cannon and Nedergaard, 2004).

2.3   Investigating organ crosstalk in humans

2.3.1   Positron emission tomography

PET/CT is a functional imaging method, which can be used for measuring tissue and organ specific metabolism *in vivo*. It is based on the administration of a radiotracer, which mimics a naturally occurring biological process. The tracer accumulates into an organ or tissue and the emitted radiation is detected with a PET camera. The data are then transformed into a 3D image, which can be visually inspected. These data can be combined with CT or magnetic resonance imaging (MRI) for further anatomical localization (Anand et al., 2009). Tissue and organ specific tracer accumulation can also be quantitated with mathematical modeling (Oikonen, n.d.). Several different organ systems and tissues can be studied *in vivo* in the same imaging session, making PET an ideal method for investigating organ crosstalk in humans.

2.3.1.1   *Principles of PET*

PET tracers (or radioligands) are produced by incorporating a proton emitting radionuclide (such as ^{15}O, ^{18}F or ^{11}C) into a biologically active molecule of interest. PET tracers are most commonly administered intravenously but can also be administered orally or by inhalation. Radionuclides are produced with a cyclotron and radioligands with very short half-lives are administered within seconds after production. After administration, the radioligand behaves according to the biologically active molecule's naturally occurring biological process.

Radionuclides steadily undergo nuclear decay, emitting protons. When a proton then collides with a nearby electron, annihilation occurs, and two gamma rays of equal energy are emitted in opposite directions. The PET scanner's detectors circle the patient and detect these pairs of gamma rays. This obtained raw data is processed in order to construct a tomographic image of the locations of annihilation events (Cherry and Dahlbom, 2006; Saha, 2010). In this way, the accumulation or high turnover of a tracer can be anatomically located.

In practice, most of the photons are not recorded, as they are either absorbed by the body or not within the field of view (FOV) of the PET scanner. Absorption is tissue specific and affected by density and volume. This loss of detection due to

absorption is called attenuation. It is important to correct attenuation with modeling, in order to prevent severe artefacts. Attenuation correction is performed by utilizing low dose CT images, acquired before the start of the PET scan.
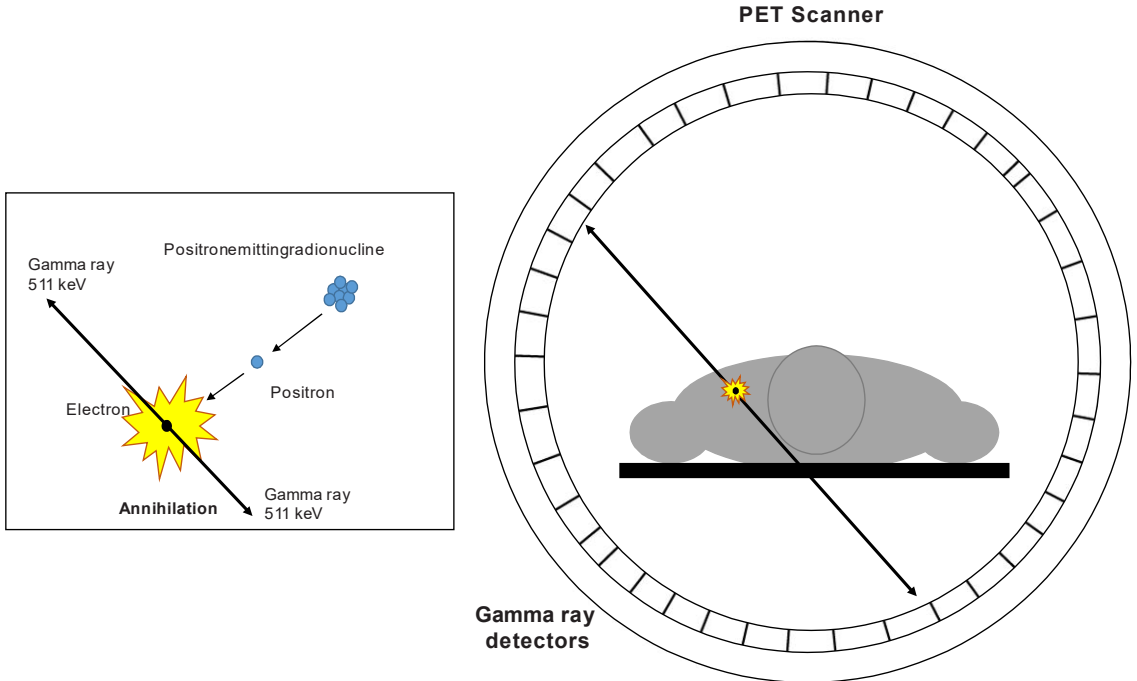

Figure 5. A positron-electron annihilation event, detected by the PET scanner. Modified from Van der Veldt et al. 2013.

2.3.1.2   Quantification of tissue metabolism with PET

There are numerous different radioligands, but [18F]FDG is the most widely available and used tracer. It is also considered the gold standard tracer for studying BAT activation (Carpentier et al., 2018). [18F]FDG mimics glucose and tissues with increased metabolism have higher glucose uptake. However, instead of going through all steps of glycolysis inside the cell, the tracer is trapped until it decays and can be detected with a PET scanner.

Standard uptake value (SUV) is a widely used, semi-quantitative method for measuring tracer uptake. It is calculated as the ratio of the image derived radioactivity concentration at a single timepoint (kBq/ml) and the whole-body concentration of injected radioactivity (MBq/kg) (Cypess et al., 2014). The benefit of this method is that it can be used for static scans, doesn't require blood sampling and is easy to implement. However, the SUV of a tissue of interest is a relative value,

directly influenced by the uptake of other tissues. This also makes it vulnerable to variation caused by factors such as muscle activity or nutritional state (Oikonen, n.d.). In the case of diagnostic [^{18}F]FDG scans, these variations can be sufficiently controlled for by patient guidance.

Due to the relative nature of SUV, quantitative measures should be preferred in scientific studies whenever possible. This requires dynamic scanning, as well as arterial sampling. In the analysis stage, a tissue specific time activity curve (TAC) is estimated from the acquired frames of the dynamic scan and an arterial input function is generated from the measured radiation of arterial samples. The net uptake rate (K_i) of a tracer can then be estimated with the graphical Patlak method (Patlak and Blasberg, 1985). In the case of [^{18}F]FDG, glucose uptake rate is calculated by multiplying K_i with plasma glucose levels and dividing the product with the lumped constant (LC). The LC is tissue specific and accounts for the transport and phosphorylation differences between glucose and [^{18}F]FDG, caused by competitive substrate kinetics (Oikonen, n.d.). Fractional uptake rate (FUR) can be used for single late scans, which is an approximation of a Patlak plot (Thie, 1995).

Tissue perfusion, or the volume of blood flowing through a volume of tissue per unit of time, can be measured with [^{15}O]H$_2$O, also called radiowater. The tracer requires an on-site cyclotron in close proximity to the PET scanner, due the radionuclide's very short half-life of 122.2 seconds. Radiowater is most commonly used to measure myocardial perfusion in order to detect ischemia, caused by obstructive coronary artery disease (Danad et al., 2014). In BAT research, is can be used to indirectly estimate BAT thermogenesis, as BAT perfusion has been shown to correlate with BAT oxygen consumption (U-Din et al., 2016). Unlike [^{18}F]FDG, [^{15}O]H$_2$O is a diffusible and inert tracer and tissue perfusion can be measured with one-tissue compartment model. Arterial input function is acquired from the PET image from inside the lumen of a large artery or the left ventricle. A direct way to measure BAT oxygen consumption is by administration of inhalable [^{15}O]O$_2$. Like [^{15}O]H2O, the tracer also requires an on-site cyclotron and equipment for automized administration. Due to the challenges of production and administration, the tracer is not in wide use.

2.3.2   Functional magnetic resonance imaging

Functional Magnetic Resonance Imaging (fMRI) is used to study neural activity. It is a non-invasive method without radiation exposure to measure brain activity at rest or during various cognitive tasks. fMRI uses the blood-oxygen-level dependent (BOLD) contrast to map changes in blood flow and oxygenation, related to energy use. These metabolic changes are associated with neural activity. When neurons become active and their demand for glucose and oxygen is increased, arterial blood

is directed to them. Oxygenated blood is less magnetic than deoxygenated blood and fMRI utilizes the differences in the magnetic properties of arterial and venous blood (Buxton et al., 2004).

Compared to PET, fMRI has superior spatial and temporal resolution, making it an ideal imaging method for studying cognitive tasks. However, various sources cause noise to the signal, such as physiological processes like respiratory movement and heartbeat, and thermal noise from both the study participant and the operating MRI system. It is also not always clear cut where the line between the signal of interest and noise goes, as the brain is often the generator of both (Liu, 2016). This is especially the case with resting state scans, where no stimulus is applied. A reaction to a single stimulus is also difficult to detect, but repeating the stimulus makes it possible to obtain a clear signal when events are averaged (Huettel et al., 2004). Implementing repeated stimulus also improves the experimental design, as experiment and control stimulus can be generated in a randomized order (Huettel et al., 2004)

3 Aims of the Study

The purpose of this study was to investigate the pleiotropic effects of the gastrointestinal hormone secretin in humans by means of imaging. Gastrointestinal hormones have recently been of interest in cardiovascular research because of their cardioprotective potential, but the effects of secretin have not been studied with modern methods. Meal induced thermogenesis and its link to appetite has not been extensively studied either. If confirmed in mouse models, conducted at the Technical University of Munich, and as proof of concept in humans studied in this thesis work, the mechanism could provide new means to treat and prevent obesity.

The specific aims of the study were:

1. To investigate whether secretin activates BAT, and secretin's potential role in initiating meal induced thermogenesis (I, II).

2. To investigate whether secretin affects appetite (I, II).

3. To investigate the effect of secretin on myocardial metabolism and kidney function in humans (III).

4 Materials and Methods

4.1 Study Subjects (I-III)

Written informed consent was provided by all subjects. The study protocol was reviewed and approved by the Ethics Committee of the Hospital District of Southwest Finland. The study was performed according to the principles of the Declaration of Helsinki. Twenty-one healthy men (n=21, mean $\pm$ standard deviation (SD), age 35.2 ± 14.4 years, BMI 23.6 ± 1.9 kg/m^2) provided data for analysis; n=15 with PET/CT (aged 41.6 ± 12.1 years, BMI 24.0 ± 1.9 kg/m^2) (I, II, III), n=5 with BAT biopsies (II), and n=14 with fMRI (aged 34.4 ± 14.6 years, BMI 23.3 ± 1.8 kg/m^2) (II). Study enrollment, participation and analysis is summarized in **Figure 6.** In addition to these participants, stored serum samples of n=17 participants of a previously reported postprandial study were analyzed for serum secretin (U-Din et al., 2018) (I).

A group of 16 participants was recruited for the PET/CT study. One participant discontinued his participation in the study after one scan and was excluded from analysis. Six participants gave additional consent to obtain supraclavicular BAT biopsies. One participant was excluded from analysis due to insufficient sample quality. After the PET/CT study, 11 participants provided written informed consent for the fMRI study. An additional group of 6 participants was recruited with the same inclusion and exclusion criteria, described below. Data from one participant was excluded from analysis due to significant protocol deviations and from two participants due to a technical failure of the MRI scanner.

Medical history, cardiovascular status, anthropometric measurements, electrocardiography (ECG), routine laboratory tests (such as hemoglobin, creatinine, amylase, and liver values), blood pressure measurements and a 2-hour oral glucose tolerance test were performed on all subjects. Inclusion criteria included BMI 20-26 kg/m^2, male sex and age 18-65 years. Exclusion criteria included current smoking, any chronic disease (such as diabetes or hyperthyroidism) or medication (such as steroids, betablockers or asthma medications) that could affect the outcome of the study or the subject's safety (such as excessive alcohol use or a history of pancreatitis).
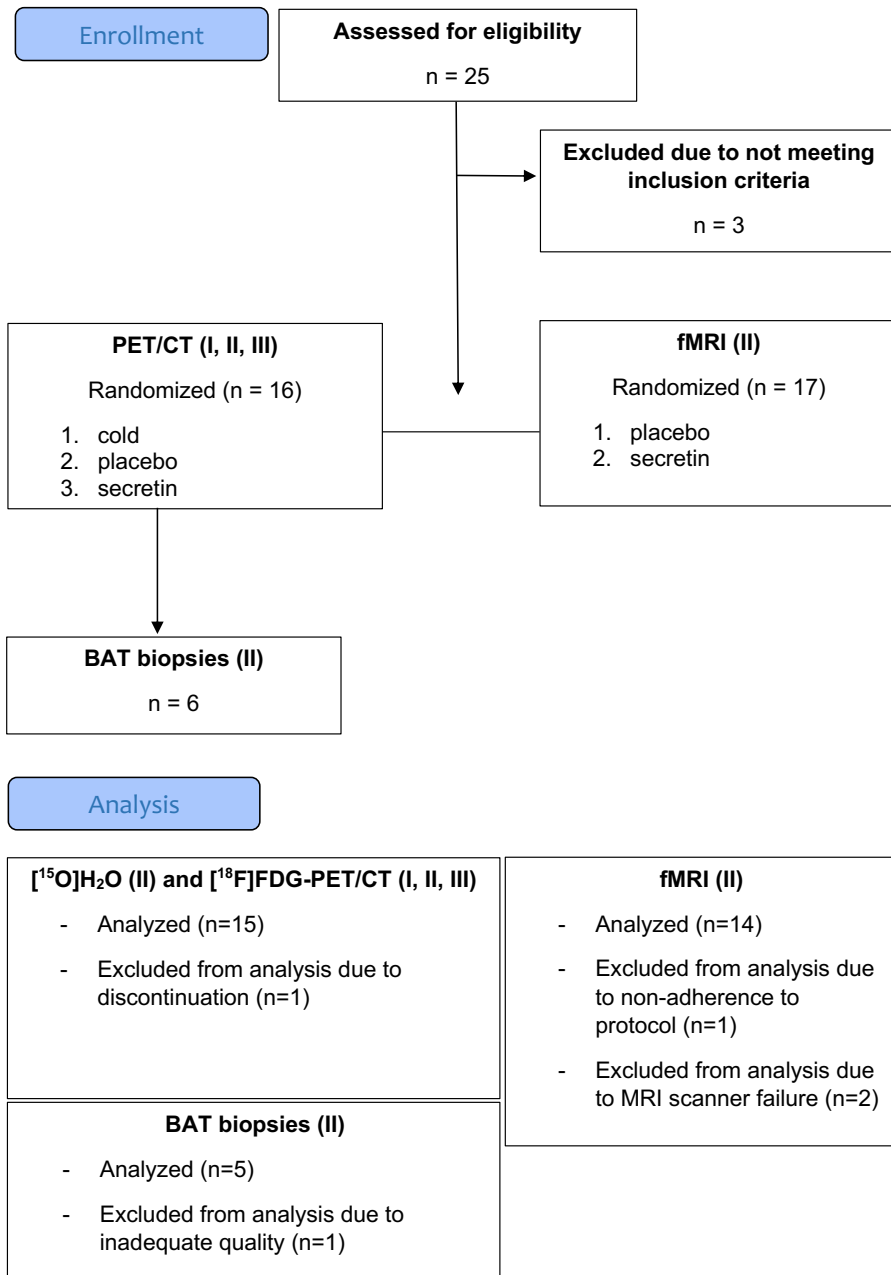
Figure 6. CONSORT flowchart on the enrolment and analysis of study subjects (I, II, III). Modified from Laurila et al. 2021.

4.2 PET-studies (I-III)

The effect of secretin on tissue perfusion and glucose uptake was investigated with PET/CT (I, II, III). The study consisted of three PET/CT scans (GE DiscoveryTM ST System, General Electric Systems, Milwaukee, MI, USA), performed on three separate days after an overnight fast (**Figure 7.**). The scans were conducted within 2-30 days of each other, in order to minimize the effects of seasonal climate variation on BAT activity (van Ooijen et al., 2004; Yoneshiro et al., 2013). One of the three scans was performed during controlled cold exposure, which was started 2 hours prior to the scan, using cooling blankets (Blanketrol III, Cincinnati Sub-Zero, Cincinnati, OH, USA) as described previously (U-Din et al., 2016). Two scans were conducted in room temperature, where subjects were single-blinded and randomized to receive intravenous infusions of placebo (saline) and secretin (secretin pentahydrochloride 1IU/kg x 2) on separate days. Whole body energy expenditure was assessed with indirect calorimeter (Deltatrac II, Datex-Ohmeda) during PET-scans (Orava et al., 2011). Conventional 12-lead electrocardiography (ECG) was recorded at baseline, one hour and two hours. Heartrate corrected QT interval (QTc) was calculated with Bazzett equation (Bazzett, 1920). Repeated arterialized venous samples were collected from the antecubital vein during scanning days.
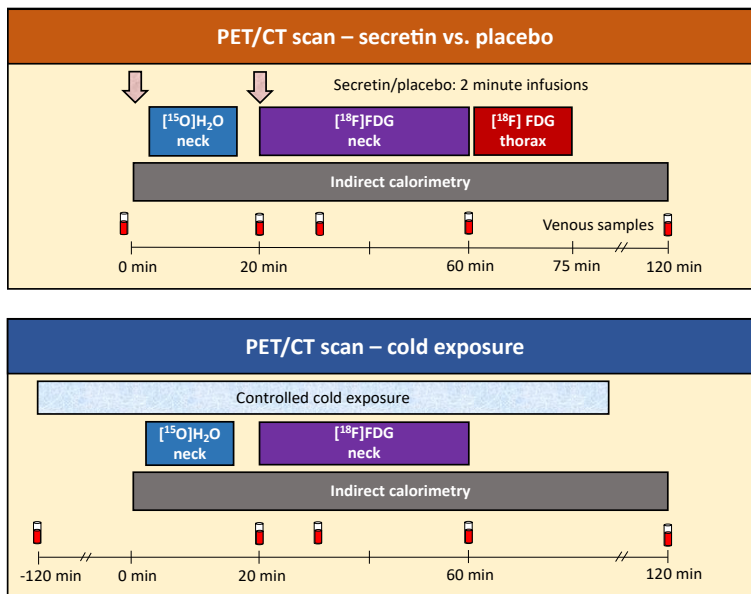
Figure 7. The PET/CT study design (I-III). Subjects (n=15) underwent three PET/CT scans: one during controlled cold exposure and two in room temperature. Subjects were randomized and single-blinded to receive secretin and placebo infusions on separate days, during room temperature scans. Infusions were given twice. All scans were conducted in the morning after an overnight fast. Red test tubes indicate timing of blood samples. Beige arrows indicate randomized secretin and placebo infusions. Modified from Laurila et al. 2021 and Laurila et al. Manuscript 2021.

4.2.1   PET image acquisition

First, a CT scan of the neck was performed for attenuation correction of PET data, and anatomic localization. On room temperature days, an intravenous infusion of placebo or secretin was then administered, after which 500 MBq of $[^{15}O]H2O$ was injected for measuring tissue perfusion (Orava et al., 2011). A dynamic six-minute scan of the neck region was acquired, using the frames 6 x 5 sec, 6 x 15 sec and 8 x 30 sec. After radioactive decay, 150 MBq of $[^{18}F]FDG$ was administered for measuring glucose uptake (GU) (Orava et al., 2011) and a second two minute infusion of placebo or secretin was initiated. Dynamic 40-minute scanning was started simultaneously on the neck region (frames: 1 x 1 min, 6 x 30 sec, 1 x 1 min, 3 x 5 min and 2 x 10 min). After the neck, the thoracic region was CT scanned for attenuation correction, then PET scanned for 15 minutes (frames: 5 x 3 min). Radiotracers were produced at the Turku PET Centre.

4.2.2   PET image analysis

Image analysis was conducted with Carimas 2.8 software (Turku PET Centre, Turku, Finland). Regions of interest (ROI) were outlined in the fusion images, composed of the dynamic $[^{18}F]FDG$ PET image and the CT image. To analyze BAT, ROIs were drawn on the supraclavicular fat depots, including only voxels with CT Hounsfield Units (HU) within the adipose tissue range (-50 to -250 HU) (U-Din et al., 2017). Skeletal muscle ROIs were drawn on the deltoid muscles. An automated cardiac analysis tool was used for the heart.

For tissue glucose uptake calculations, TACs were generated for the ROIs. Regional TAC data was analyzed by taking into account the radioactivity in arterialized plasma, using the Patlak model (Patlak and Blasberg, 1985) for BAT and deltoid muscles and FUR (Thie, 1995) for the heart. Arterialized plasma radioactivity was assessed with an automatic gamma counter (Wizard 1480, Wallac, Turku, Finland). A lumped constant value of 1.14 was used for adipose tissue (Virtanen et al., 2001), 1.20 for skeletal muscle (Peltoniemi et al., 2000) and 1 for the myocardium (Bøtker et al., 1997).

For radiowater BAT analysis, arterial input function was determined by drawing a ROI in the arch of aorta. The same BAT ROIs from the $[^{18}F]FDG$ images were used for the analysis of BAT perfusion. Perfusion was calculated using the one-tissue compartment model, as previously described (U-Din et al., 2016).

4.3   Indirect Calorimetry (II, III)

Whole body energy expenditure was assessed with indirect calorimetry during PET-scans, as described previously (U-Din et al., 2016). The first minutes of calorimetry data were excluded to measure the steady state, and analysis started from 10 minutes after the first secretin dose. Whole body energy expenditure and the rate at which carbohydrates and lipids were oxidized for it, were calculated with Matlab (Version: R2011a), using the Weir equation (Weir, 1949) and the manufacturer's equations (Meriläinen, 1987). Protein metabolism was calculated by assuming urine nitrogen as 13 g/24h.

4.4   fMRI studies (II)

The second part of the study consisted of two separate fMRI scans (3-Tesla Philips Ingenuity PET/MR scanner) performed in the morning after an overnight fast at room temperature with identical protocols. Again, the individual scans were performed within 7-30 days, in order to minimize seasonal effects on appetite and BAT function. As in the metabolic PET/CT studies, secretin and placebo were administered in a randomized fashion, where subjects were blinded to the intervention. Food cue tasks were initiated after the second infusion, timed to correspond the timing of the $[^{18}F]$FDG PET/CT scan of the neck region. Satiety was assessed by measuring composite satiety score by visual analogue scale questions during scan days. The amount of food eaten after the scan was documented at the study center. Subjects filled in food diaries two days prior to, during, and three days after the study day.
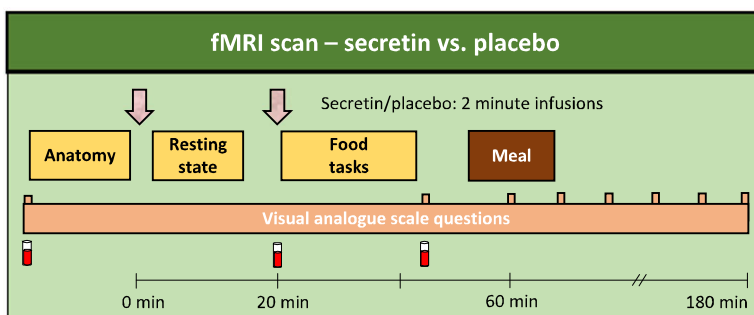
Figure 8. fMRI study design (II). Subjects (n=14) underwent two fMRI scans, where they were randomized and single-blinded to receive secretin and placebo infusions on separate days. After scanning, subjects had a meal and were then followed up for two hours. Subjective measurements on appetite were collected with visual analogue scale questionnaires at prespecified timepoints. All scans were conducted in the morning after an overnight fast. Beige arrows indicate randomized secretin and placebo infusions. Modified from Laurila et al. 2021.

4.4.1   fMR tasks and image acquisition

A previously established task protocol (Nummenmaa et al., 2018) was implemented for inducing anticipatory reward, by showing the participants pictures of palatable (e.g. chocolate, pizza, cakes), and non-palatable (e.g. lentils, cereal, eggs) foods (**Figure 9.**). This task simulates situations where appetite is triggered by anticipating the actual feeding via visual food cues, such as those in advertisements. The pictures were rated in a previous study by independent participants; the ratings showed that the palatable foods were evaluated more pleasant than the non-palatable foods (Nummenmaa et al., 2012).

During the tasks, functional data were acquired with gradient echo-planar imaging (EPI) sequence, sensitive to the BOLD signal. Participants viewed alternating 16.2-s epochs with pictures of palatable or non-palatable foods. Each epoch contained nine stimuli from one category, intermixed with fixation crosses. Each food stimulus was presented on either the right or the left side of the screen, and participants were instructed to indicate its location by pressing corresponding buttons. This task was used simply to ensure that participants had to pay attention to the stimuli. Stimulus delivery was controlled by the Presentation software (Neurobehavioral System, Inc., Berkeley, CA, USA).

Functional data were acquired using 3-Tesla Philips Ingenuity PET/MR scanner and using EPI sequence with the following parameters: TR = 2600 ms, TE = 30 ms, flip angle 75°, 240 x 240 x 135 mm FOV, $3 \times 3 \times 3$ mm voxel size. Each volume consisted of 45 interleaved axial slices acquired in ascending order. A total of 165 functional volumes were acquired, with additional five dummy volumes acquired and discarded at the beginning of each run. Anatomical reference images were acquired using a T1-weighted sequence with following parameters: TR 8.1 ms, TE 3.7 ms, flip angle 7°, 256 x 56 x 176 mm FOV, $1 \times 1 \times 1$ mm voxel size.
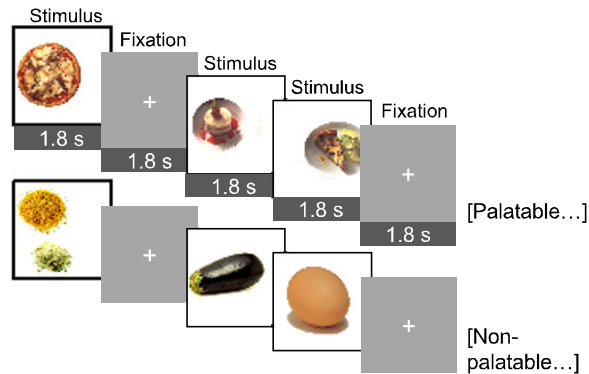
Figure 9. fMRI paradigm where pictures of palatable vs. non-palatable foods were presented to study subjects under secretin or placebo conditions. The protocol included twelve 16.2 second blocks with palatable or non-palatable foods; 6 food stimuli intermixed with 3 fixations in one block. Modified from Laurila et al. 2021.

4.4.2 fMRI analysis

Pre-processing of MRI images was performed using FMRIPREP (version 1.3.0.2) (Esteban et al., 2019), a Nipype (version 1.1.9) (Gorgolewski et al., 2011) based tool. Each T1-weighted image was corrected for intensity non-uniformity with N4BiasFieldCorrection (version 2.1.0) (Tustison et al., 2010) and skull-stripped based on the OASIS template with antsBrainExtraction.sh workflow (ANTs version 2.2.0). Brain surfaces were reconstructed using recon-all from FreeSurfer (version 6.0.0) (Dale et al., 1999), and the brain mask estimated previously was refined with a custom variation of the method to reconcile ANTs- and FreeSurfer-derived segmentations of the cortical grey matter, using Mindboggle (Klein et al., 2017). Spatial normalization to the ICBM 152 Nonlinear Asymmetrical template version 2009c (Fonov et al., 2009) was done with nonlinear registration, using the antsRegistration tool (Avants et al., 2008). Tissue segmentation of cerebrospinal fluid, white-matter and grey-matter was performed on the brain-extracted T1w using fast (Zhang et al., 2001) of FSL (version 5.0.9). Functional MRI images were slice time corrected with 3dTshift from AFNI (version 16.2.07) (Cox, 1996) and motion corrected with mcflirt (Jenkinson et al., 2002) from FSL. This was followed by co-registration to the corresponding T1w via boundary-based registration (Greve and Fischl, 2009) with nine degrees of freedom, using bbregister from FreeSurfer. These steps were concatenated and applied in a single step via antsApplyTransforms with the Lanczos interpolation. Physiological noise regressors were obtained using CompCor (Behzadi et al., 2007), where principal components were estimated for temporal and anatomical variants. A mask to exclude signal with cortical origin was created via eroding the brain mask, ensuring it originated merely from subcortical structures. Six temporal CompCor components were then calculated, including the

top 5% variable voxels within that subcortical mask. For anatomical CompCor components, six components were calculated within the intersection of the subcortical mask and the union of cerebrospinal fluid and white matter masks, after projection to the native space of each functional run. Frame-wise displacement (Power et al., 2014) was calculated for each functional run, using the implementation of Nipype. Finally, ICA-based Automatic Removal Of Motion Artifacts (AROMA) was used to generate aggressive noise regressors, and also to create a variant of data which is non-aggressively denoised (Pruim et al., 2015).

4.5 Appetite and feeding (II)

4.5.1 Composite satiety score

Satiety was assessed during the study days by measuring composite satiety score (CSS), by utilizing a validated visual analogue scale (VAS) questionnaire (Flint et al., 2000; Gilbert et al., 2012) to calculate CSS (CSS = satiety + fullness + (100 − prospective food consumption) + (100 − hunger)) (**Figure 10.**). All questions were answered in Finnish. Subjects filled in the questionnaire in three different phases of the study: pre-prandial (at baseline and after the scan), prandial (ten minutes into feeding) and postprandial phase (directly after feeding, then every 30 minutes up to 2 hours after feeding).
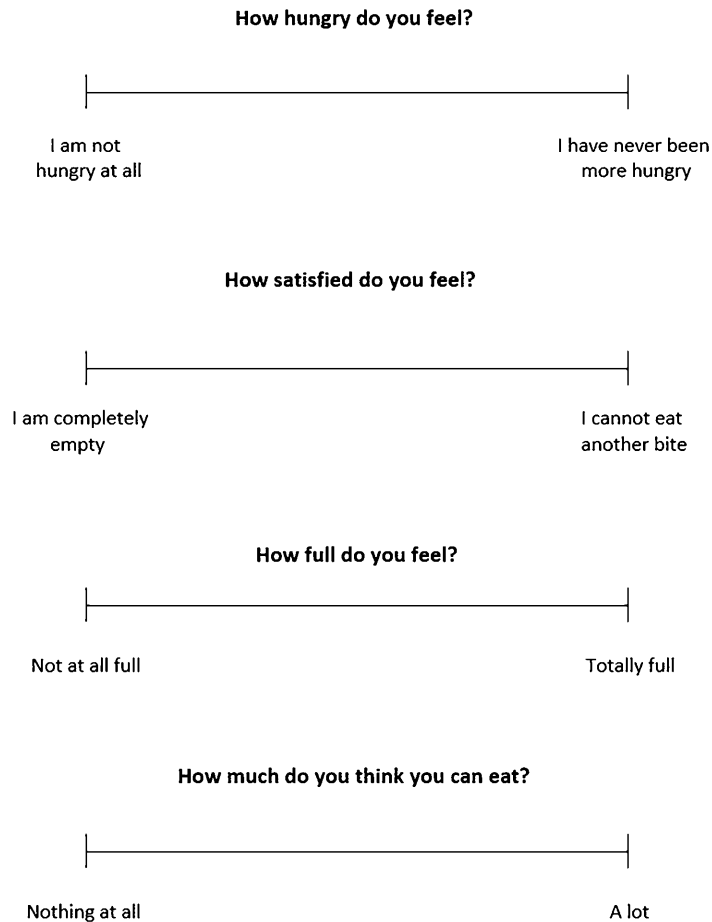
How hungry do you feel?

|—————————————————————————————|

I am not   I have never been
hungry at all   more hungry

How satisfied do you feel?

|—————————————————————————————|

I am completely   I cannot eat
empty   another bite

How full do you feel?

|—————————————————————————————|

Not at all full   Totally full

How much do you think you can eat?

|—————————————————————————————|

Nothing at all   A lot

Figure 10. Visual analogue scale questionnaire (II). Modified from Laurila et al. 2021.

4.5.2   Dietary intake

Subjects were instructed to eat and live normally before the scanning days, avoiding heavy exertion and events that involve excessive feeding or alcohol consumption. Subjects were also instructed to pay attention to eating similar foods at similar time points the day before both fMRI scans. Food diaries were checked for compliance with instructions. Fasting was instructed to begin at 10 p.m. the previous night and continued until the scan. All fMRI scans were conducted between 8 a.m. and 11 a.m.

After the fMRI scan, subjects were offered a standardized meal (one kilogram of pasta and minced meat casserole, with the energy content of 102.86 kcal per 100 grams) and advised to eat at their own pace until they felt satiated. Subjects ate at the PET Centre kitchen without outside disturbances for 20 minutes. They filled in a VAS questionnaire and the food container was weighed at 10 min and 20 min after

start of meal, to assess whether secretin has an effect on the size of the first meal after an overnight fast. Food diaries were utilized to calculate the effect of secretin compared to placebo on the resumption to eat after the first meal.

4.6   Serum and plasma measurements (I-III)

During PET/CT scans, blood samples were collected from the antecubital vein through a cannula at baseline and after 10 min, 20 min, 30 min, 60 min and 120 min from start of scan (**Figure 7.**). Plasma samples were collected at baseline, 20 min, 30 min, 60 min and 120 min. Serum samples were analyzed for metabolites (such as serum total fatty acids and creatinine) at Nightingale laboratory with nuclear magnetic resonance (NMR) spectroscopy (Soininen et al., 2009). Plasma samples for glucose and insulin were analyzed with electrochemiluminescence immunoassays (ECLIA) at the Turku University Hospital laboratory. Serum secretin levels were determined by enzyme-linked immunosorbent assay (ELISA), using a kit purchased from Cloud-Clone, following the manufacturer's instructions. Secretin concentrations were calculated using a standard curve generated by secretin standards included in the kit.

4.7   BAT biopsies (II)

Biopsies were obtained in non-fasting state on a separate, late afternoon visit (n=6). Supraclavicular BAT depots were localized using cold exposure PET/CT scans. BAT samples were collected in local anesthesia, with lidocaine c. adrenalin (10 mg/ml + 10 μg/ml), from a single incision by an experienced plastic surgeon, under the supervision of an anesthesiologist. Samples were preserved in formalin and immunohistochemistry for SCTR detection was performed at the Technical University of Munich (TUM).

4.8   Renal function measurements (III)

For urine secretion measurements, subjects voided before and after the PET/CT scan. Times were recorded and urine volumes measured. Urine radioactivity after the [18F]FDG scan and arterialized plasma sample radioactivity, measured at previously described timepoints (**Figure 7.**), were assessed with an automatic gamma counter (Wizard 1480, Wallac, Turku, Finland). [18F]FDG renal clearance rate was calculated as previously described, with urine activity (FDG_{urine}) divided by area under the curve (AUC) arterialized plasma radioactivity from beginning of the scan to the end (Latva-Rasku et al., 2019).

$$Renal\ Clearance_{FDG} = FDG_{urine} \Big/ AUC_{0 \to sampling\ time}$$

Estimated glomerular filtration rate (eGFR) was measured with Cockcroft-Gault equation (Cockcroft and Gault, 1976), calculated from serum creatinine measurements.

$$Creatinine\ Clearance_{male} = ([140 - age] \times kg) \Big/ (serum\ creatinine \times 72)$$

4.9 Preclinical studies (I)

Preclinical studies were conducted by our collaborators at the Technical University of Munich. Mice were bred at the animal facility of the Technical University of Munich. The animals were housed at $22\pm1°C$ and 50-60% relative humidity in a 12h:12h light:dark cycle and they had *ad libitum* access to food and water. All animal experiments were approved by the German animal welfare authorities at the district government.

RNA sequencing was performed on BAT samples of n=4 male C57BL/6J mice. Libraries from all samples were pooled and then sequenced. All genes and transcripts were assigned relative coverage rates as measured in RPKM units (reads per kilobase per million mapped reads). *In vivo* experiments were conducted on 129S1 mice for WT vs. UCP1 KO experiments, and 129S6 for noradrenaline vs. secretin experiments. Mice were kept at thermoneutrality (30°C) for 1 week prior to indirect calorimetry measurements. Intraperitoneal injections of (5 nmol) secretin, equal volume of placebo or noradrenalin (1 mg/kg) was administered, and indirect calorimetry was measured for 1 hour. For direct visualization of BAT activation by 5 nmol of secretin, athymic, female Nude-Foxn1[nu] mice were studied with indirect calorimetry, coupled with multispectral optoacoustic tomography (MSOT) (n=6). Heat production, total blood volume in the Sulzer vein and oxygen saturation was measured before and after secretin administration. MSOT enables the quantification of oxygenated and deoxygenated hemoglobin. Total blood volume was assessed as the sum of oxygenated and deoxygenated hemoglobin. To monitor intrascapular BAT (iBAT) temperature, 129S6/SvEv mice were anesthetized, and telemetry transmitters were implanted above the iBAT pad. Cumulative food intake was measured up to 3 hours in WT and UCP1 KO 129S1/SvEv mice after overnight (18h) fasting. The neurobiological basis for a satiation effect was then investigated by measuring the relative expression abundance of mRNAs of interest from hypothalamic samples. The hypothalamus of fasted WT and UCP1 KO mice was removed 4 hours after intraperitoneal injections of secretin 5nm or placebo.

4.10   Statistical analysis (I-III)

Data are reported as means $\pm$ SD for normally distributed data and medians $\pm$ interquartile range (IQR) otherwise. Statistical analysis for animal studies was conducted with GraphPad Prism8 (I), for PET/CT, calorimetry, food diary and urine measurement data with IBM SPSS Statistics (versions 25 and 27) (II, III) and for serum metabolites, plasma hormones and composite satiety score, with R-studio (II, III). Student's t-test was used to compare changes within subjects, when differences were normally distributed, and paired Wilcoxon signed-rank test when not normally distributed. Independent samples T-test was used to compare two different groups. Correlations were analyzed with Pearson's correlation for linear and Spearman's rank correlation for non-linear associations between paired observations. For analysis of multiple timepoints, placebo and secretin interventions were compared using paired Wilcoxon test for each timepoint and AUC. P-values are marked as * $p<0.05$, ** $p<0.01$, *** $p<0.001$.

Functional MRI data was analyzed using SPM12 (version 7487) run with Matlab (version R2016b). In the analysis, the whole-brain random effects model was applied, using a two-stage process with separate first and second level. For each participant, the general linear model was first used to predict regional effects of task parameters (palatable and non-palatable foods) and drug condition (secretin, placebo) on BOLD indices of activation. Subject-wise contrast images were generated for the effect of palatable versus non-palatable foods in the secretin and placebo conditions, as well as interaction effect between food categories and conditions, and subjected to second-level analyses. The resulting statistical images were thresholded at $p<0.05$, false discovery rate (FDR) corrected.

5   Results

5.1   Secretin activates BAT (I, II)

Secretin had the highest transcription levels in murine brown adipose tissue out of all investigated gut hormone receptors (**Figure 11A.**). Thus, we hypothesized that secretin activates BAT. SCTR was thereafter confirmed in n=5 human study participant BAT biopsies by immunohistochemistry (**Figure 11B.**).
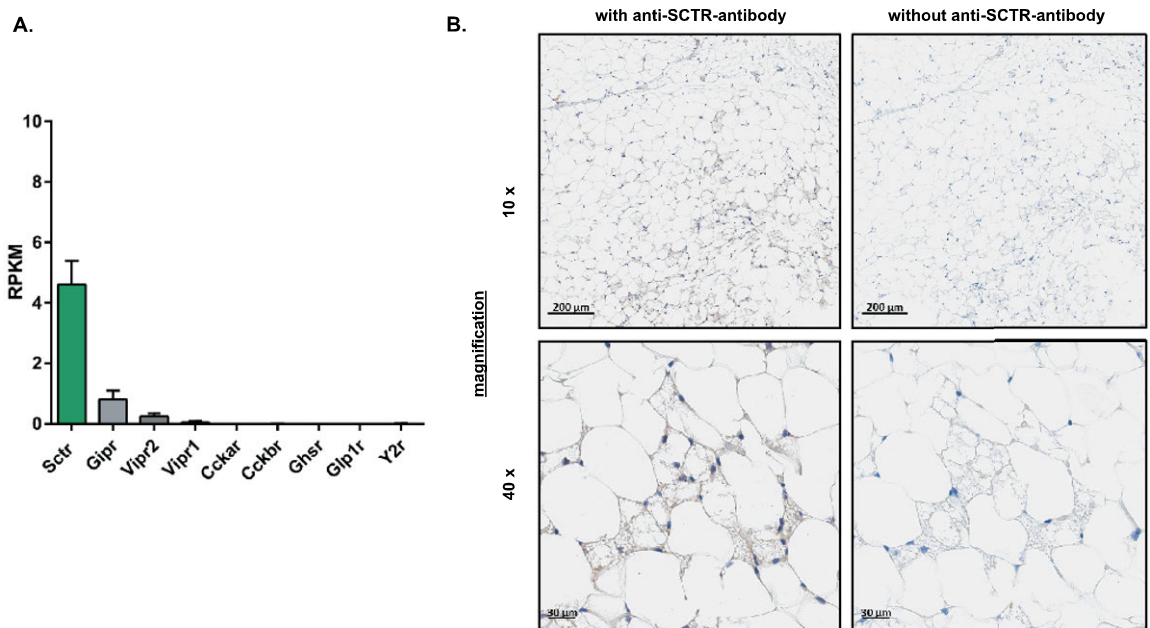

Figure 11. A. Expressed gut hormone receptors in murine interscapular brown adipose tissue as RPKM (reads per kilobase per million mapped reads). Secretin receptor (Sctr) has the highest transcript abundance, compared to gastric inhibitory polypeptide receptor (Gipr), vasoactive intestinal peptide receptor1/2 (Vipr1/2), Cholecystokinin A/B receptor (Cckar/br), Ghrelin receptor (Ghsr), glucagon-like peptide 1 receptor (Glp1r) and the PYY receptor (Y2r). (I) **B.** Immunohistochemical detection of secretin receptor (SCTR) in human supraclavicular brown adipose tissue (nuclei stain haematoxylin; magnification: x 10 and x 40; scale bars, 200µm and 30 µm). (II) Modified from Li et al 2018 and Laurila et al. 2021.

Secretin was shown to induce non-adrenergic, UCP1 mediated thermogenesis in cultured mouse primary brown adipocytes. Thermogenesis was then investigated *in vivo* by indirect calorimetry. In WT mice, kept at thermoneutral conditions (30°C) one week prior to measurements, an intraperitoneal injection of secretin induced a rise in heat production, comparable to noradrenaline (**Figure 12A.**). Whole body energy expenditure was also increased by intravenous secretin compared to placebo in human participants (**Figure 12B.**).
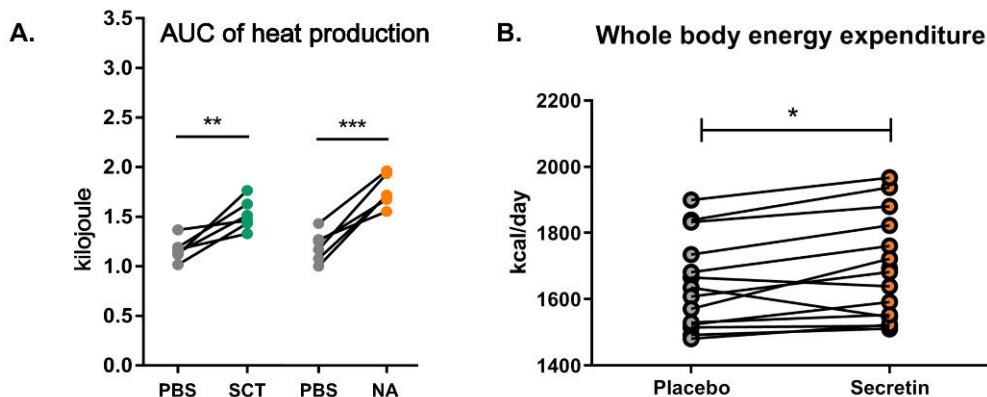

Figure 12. A. Area under the curve (AUC) heat production in wild type mice, measured for one hour by calorimetry after placebo (PBS), secretin (SCT) and noradrenaline (NA) administration at 0 minutes (n=6). (I) **B.** Whole body energy expenditure in human participants, measured for two hours by indirect calorimetry, after placebo and secretin administration at 0 and 20 minutes (n=15). (II) Modified from Li et al. 2018 and Laurila et al. 2021.

In order to investigate brown adipose tissue thermogenesis *in vivo*, the venous drainage of interscapular BAT was monitored in nude mice. Heat production, total blood volume and oxygen consumption of BAT was increased by secretin compared to placebo (**Figure 13A.**). In human participants, secretin increased BAT GU compared to placebo (**Figure 13B.**), while BAT perfusion was not changed (mean $\pm$ SD, secretin vs. placebo, 4.84 ± 1.85 ml/100g/min vs. 6.00 ± 3.12 ml/100g/min, ns). BAT GU after secretin did not correlate with cold induced BAT GU (r=-0.107, p=0.704), supporting that secretin induced BAT activation is non-adrenergic in humans as well, unlike cold activation.
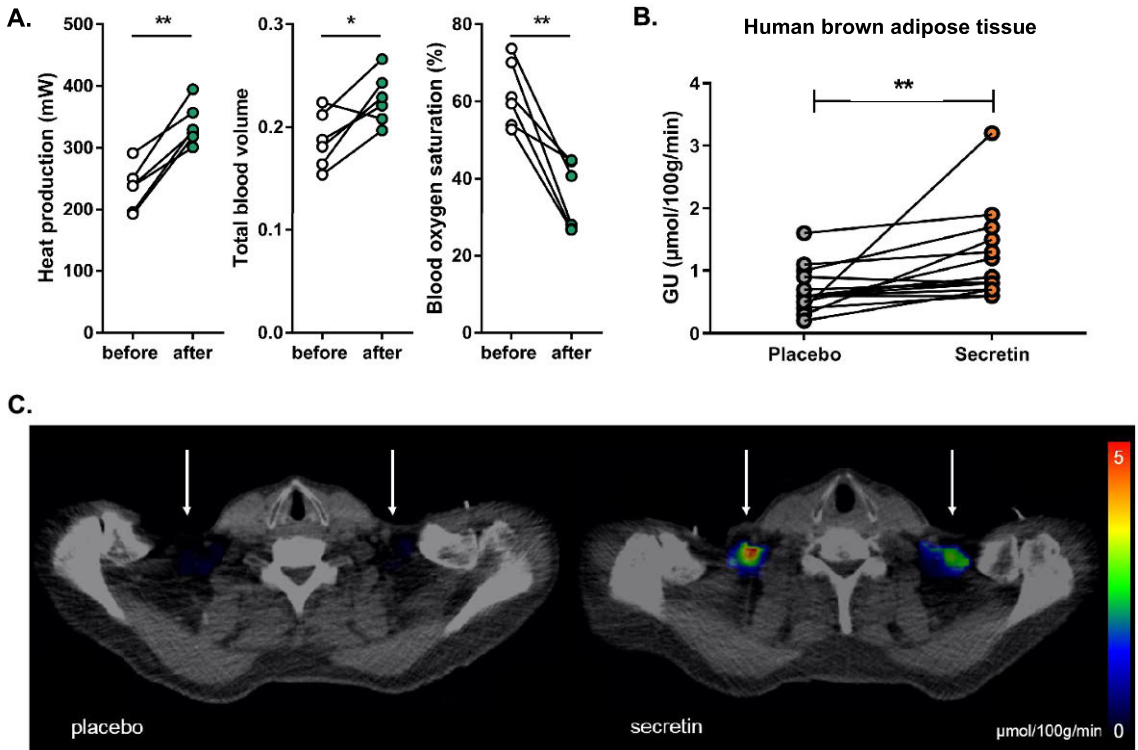
Figure 13. A. Murine brown adipose tissue heat production, and total blood volume and blood oxygen saturation in the Sulzer vein before and after 5 nmol of secretin, measured through indirect calorimetry coupled with multispectral optoacoustic tomography in nude mice (n=6). (I) **B.** Human brown adipose tissue glucose uptake (GU) after placebo and secretin (2 x 1 IU/kg) infusion (n=15). (II) **C.** Representative parametric PET/CT images of brown adipose tissue glucose uptake after placebo and secretin (II). Modified from Y. Li et al. 2018 and Laurila et al. 2021.

Lastly, the role of secretin and postprandial thermogenesis was studied in mice and men. Plasma secretin levels were confirmed to increase postprandially from fasting levels (**Figure 14A+B.**) and a concomitant increase in interscapular brown adipose tissue temperature was shown in mice (**Figure 14C.**). Pre- and postprandial secretin levels were measured in a group of subjects, who participated in a previously reported study on postprandial BAT activation (U-Din et al., 2018). After a mixed meal, BAT oxygen uptake (**Figure 14D.**) and fatty acid uptake (n=16) (r=0.621, p=0.010) was associated with serum secretin levels.
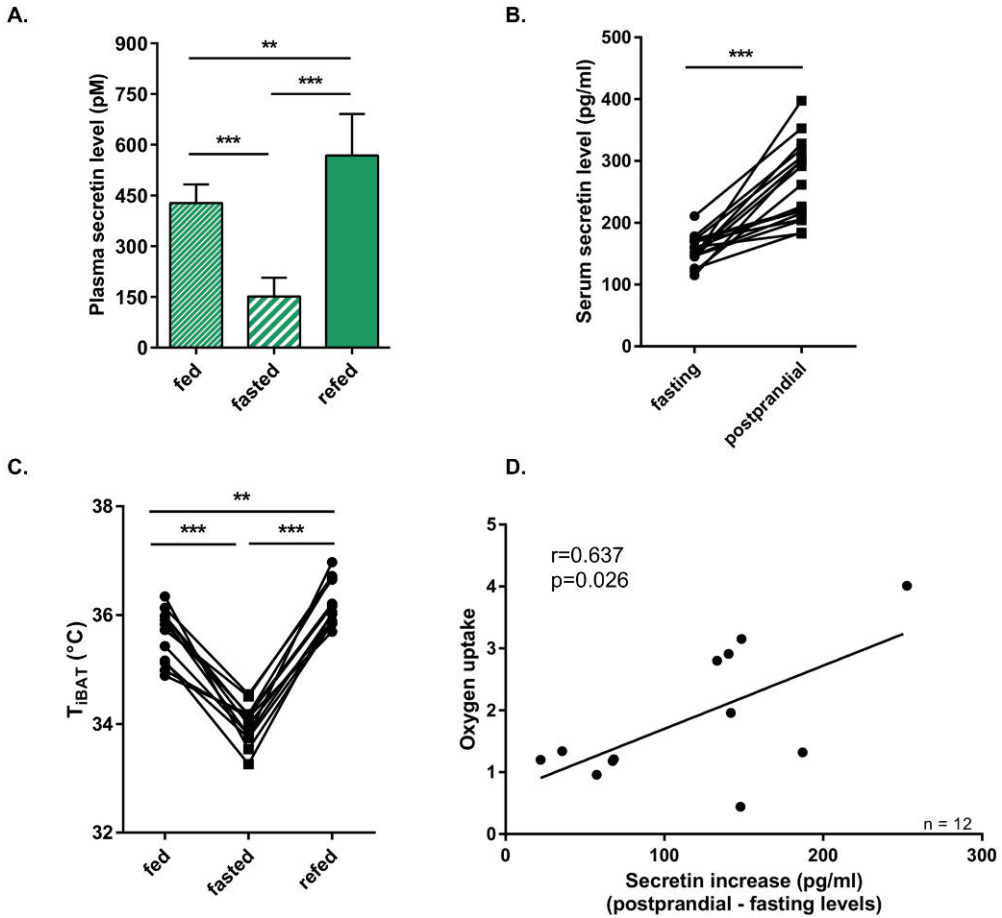
A.

Figure 14. **A.** Plasma secretin levels in fed, fasted and refed mice (n=6). (I) **B.** Serum secretin levels in fasting conditions and after a mixed meal in n=17 men. (I) **C.** The temperature of interscapular BAT in fed, fasted and refed mice (n=12). (I) **D.** Correlation between BAT oxygen uptake and serum secretin levels after a mixed meal in n=12 men. (I) Modified from Li et al. 2018.

5.2 Secretin induces satiation (I, II)

Secretin's effect on food intake was first studied on WT mice by our collaborators. Compared to placebo, a 5 nmol intraperitoneal injection of secretin decreased food intake in prandial and early postprandial, but not in the late postprandial phase (2-3 hours after the injection) (**Figure 15A.**). Remarkably, reduction of food intake was only seen in WT mice and not UCP1 KO mice, indicating that the satiation effect is mediated through BAT thermogenesis (**Figure 15B.**). Furthermore, intermeal bouts were shorter in UCP1 KO mice, compared to WT mice (**Figure 16B.**). When WT mice were treated with a secretin antibody to neutralize endogenous secretin, meal

duration and meal size was significantly increased compared to controls (**Figure 16A.**).

Secretin's effect on appetite was thereafter studied in human participants. Intravenous secretin (1 IU/kg x 2) increased satiety compared to placebo, according to CSS AUC in the pre-prandial and prandial phase (**Figure 15C.**), but not postprandially (mean $\pm$ SD secretin, vs. placebo, 311.3 $\pm$ 136.1 vs. 266.2 $\pm$ 126.4, p=0.130). Even if secretin did not reduce meal size statistically significantly (mean $\pm$ SD, secretin vs. placebo, 489.0 $\pm$ 109.4 kcal vs. 522.0 $\pm$ 167.5 kcal, p=0.273), it delayed resumption to refeed (**Figure 16C.**).

The neurobiological basis of secretin's satiation effect was investigated in fasted WT and UCP1 KO mice. In WT mice, secretin increased the anorexigenic proopiomelanocortin (POMC) mRNA levels in the hypothalamus (**Figure 17B.**). Concomitantly, the orexigenic agouti-related protein (AgRP) mRNA levels also decreased (**Figure 17A.**). Furthermore, the expression of a temperature sensitive ion channel, transient receptor potential vanilloid 1 (TRPV1) (also known as capsaicin receptor), was upregulated in the POMC neurons of WT mice but not UCP1 KO mice (**Figure 17C.**).

Secretin's central effects on appetite were thereafter investigated in human participants by fMRI. After placebo, palatable food in contrast to non-palatable food led to increased hemodynamic activity in the brain reward circuits (**Figure 17D.**). These results are in line with previous studies (Nummenmaa et al., 2018). Remarkably secretin essentially abolished this anticipatory reward-sensitive coding (**Figure 17D.**).
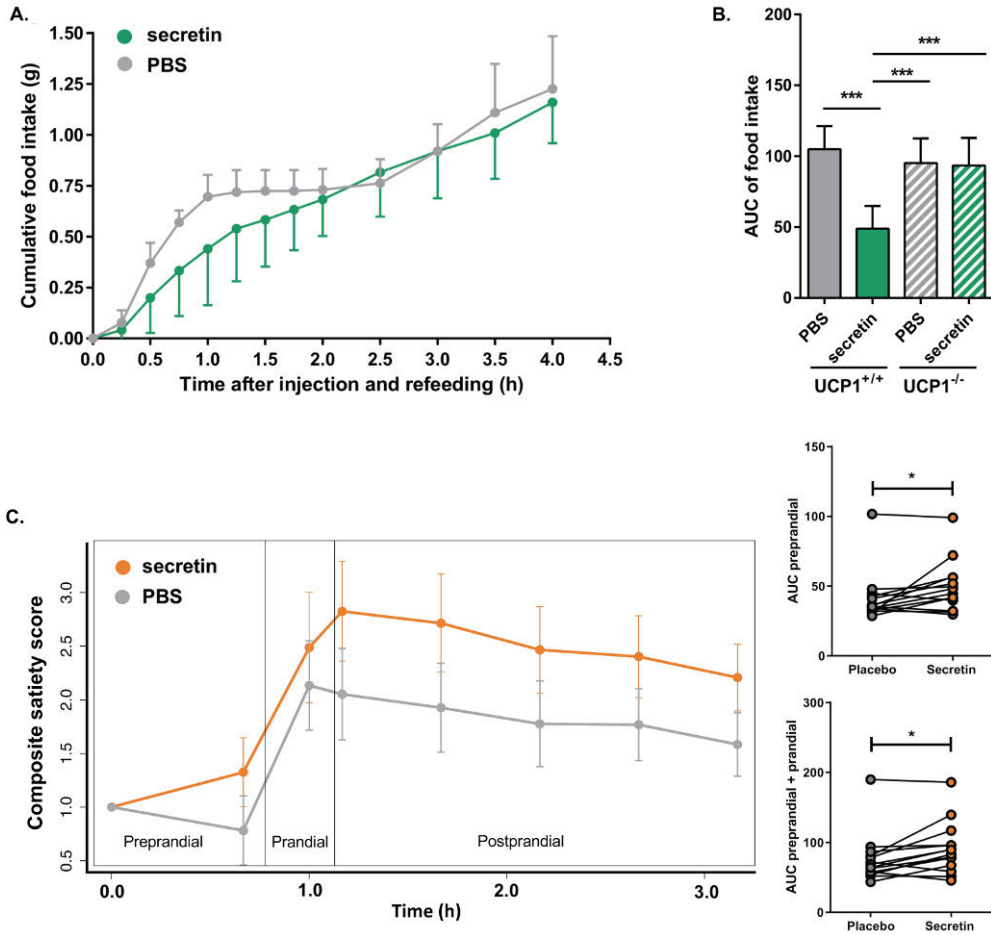
Figure 15. A. An intraperitoneal injection of secretin or placebo was given to fasted wild type (UCP1$^{+/+}$) mice and cumulative food intake was measured (n=6). (I) **B.** Cumulative food intake by area under the curve (AUC) in UCP1$^{+/+}$ and UCP1 knockout (UCP1$^{-/-}$) mice after secretin and placebo (n=6). (I) **C.** Secretin and placebo was administered twice to fasted human participants and composite satiety score (CCS) was measured with visual analogue scale questions (n=14). Functional magnetic resonance imaging was conducted in the pre-prandial phase, after which subjects ate casserole until satiated (prandial phase). Satiety was increased in the pre-prandial and prandial phase, calculated by AUC. (II) Modified from Li et al. 2018 and Laurila et al. 2021.
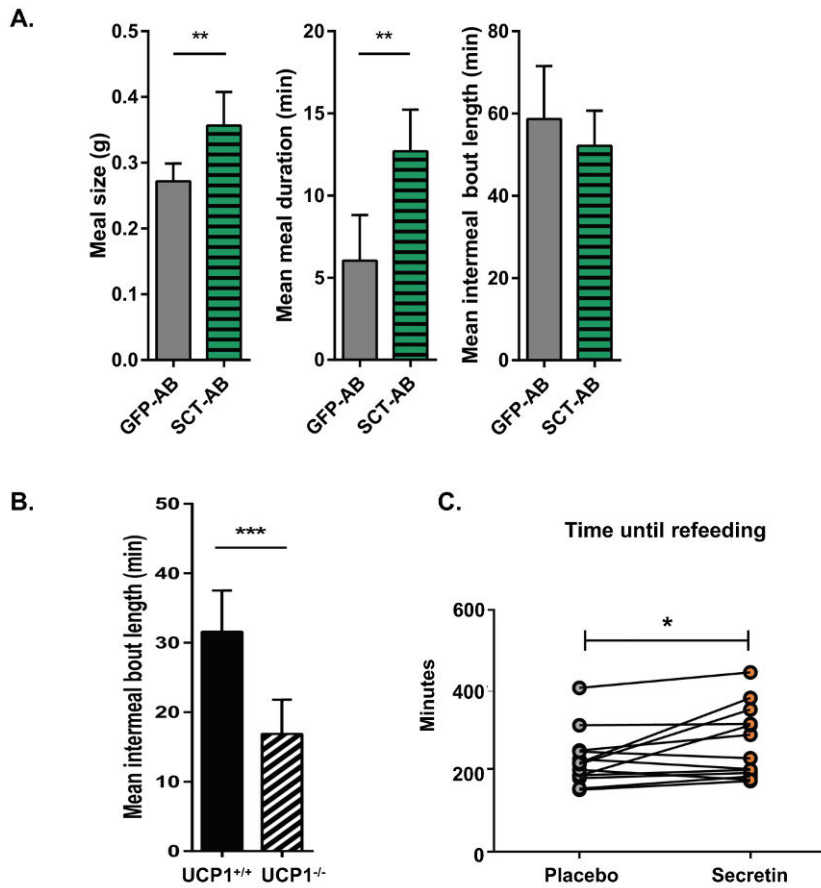
Figure 16. A. Wild type mice (UCP1$^{+/+}$) were treated with a secretin antibody (n=6) and as controls, a GFP antibody (n=6). When endogenous secretin was neutralized, meal size and mean meal duration was increased significantly. (I) **B.** Mean intermeal bout length was increased in n=6 UCP1$^{+/+}$ mice during dark phase, compared to n=6 UCP1 knockout mice (UCP1$^{-/-}$). (I) **C.** In n=14 human participants, time until refeeding was increased after intravenous secretin compared to placebo. (II) Modified from Li et al. 2018 and Laurila et al. 2021.
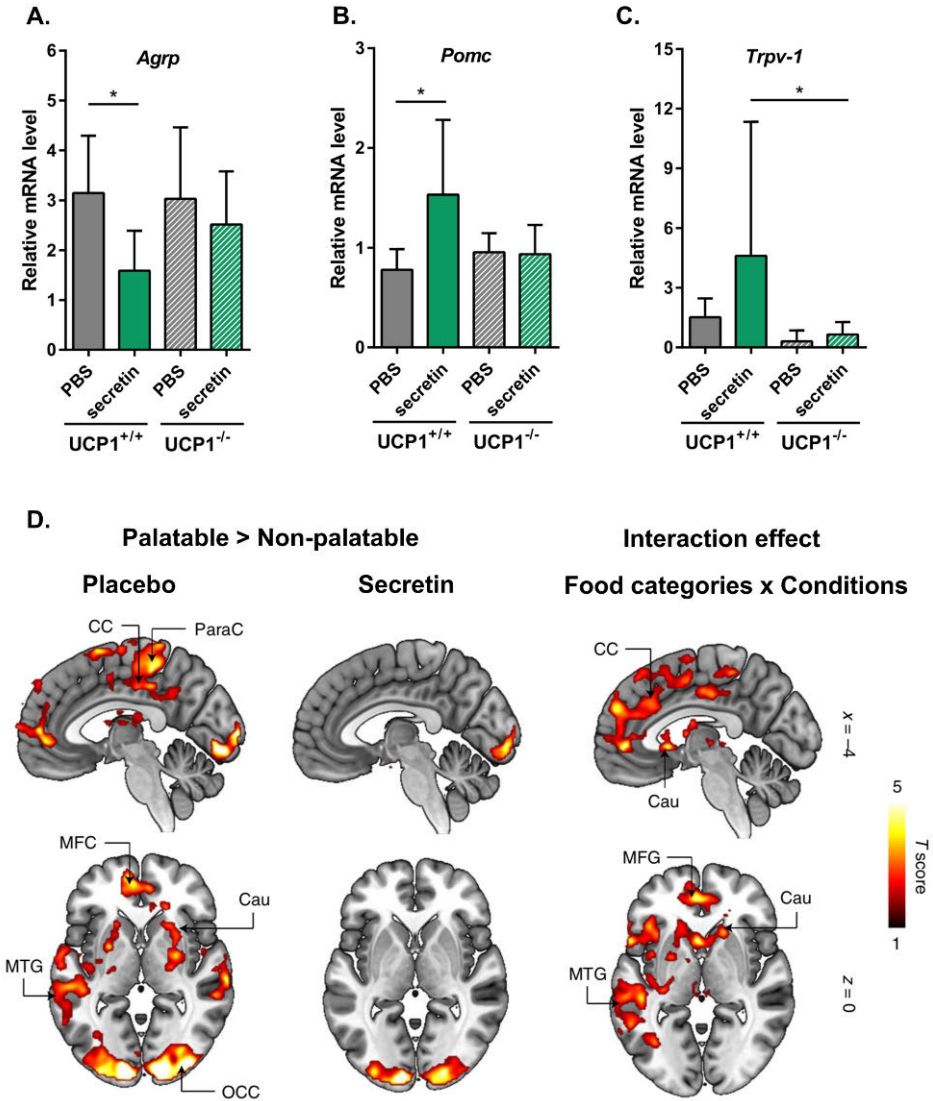
Figure 17. Relative mRNA levels of **A.** the orexigenic, agouti related peptide (AgRP), **B.** anorexigenic proopiomelanocortin (Pomc) and **C.** heat sensing capsaicin receptors (Trpv-1) in the hypothalamus of wild type (UCP1$^{+/+}$) and UCP1 knockout (UCP1$^{-/-}$) mice after placebo and secretin. (I) **D.** fMRI results of human participants (n=14). After placebo, hemodynamic activity was increased in reward circuits while viewing palatable vs. non-palatable foods. Secretin diminished this activity. An interaction effect between food categories and drug intervention is present in the same brain areas, indicating secretin-dependent changes. Data was thresholded at p<0.05 and FDR corrected. MFC = medial frontal cortex, CC = cingulate cortex, PCC = posterior cingulate cortex, OCC = occipital cortex, Cau = caudate, Ins = insula, MTG = middle temporal gyrus. (II) Modified from Li et al. 2018 and Laurila et al. 2021.

5.3 Secretin increases myocardial metabolism, renal function and serum fatty acids (II-III)
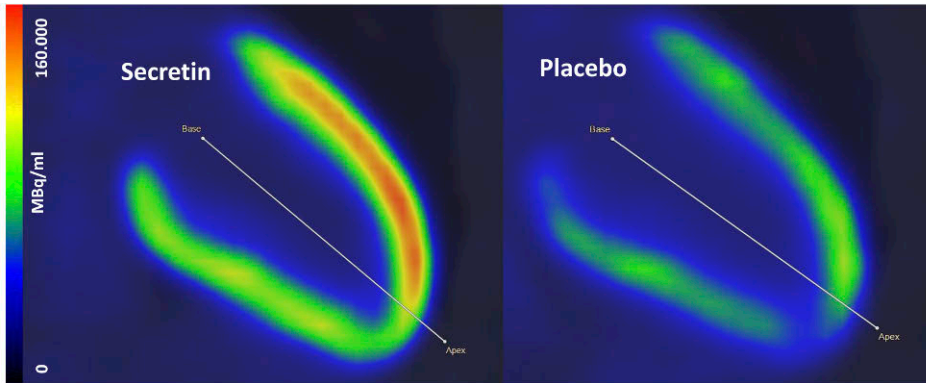
Myocardial glucose uptake (MGU) was significantly increased with secretin compared to placebo (**Figure 18A+B.**). Furthermore, MGU was associated with whole body carbohydrate oxidation during the secretin intervention (**Figure 18C.**). There was no significant difference in heart rate between the interventions at the start of the thoracic scan (57 ± 8 beats per minute (bpm) vs. 57 ± 8 bpm, p=0.92), but QTc was shortened after secretin compared to placebo (410.2 ± 26.1 ms vs. 417.0 ± 21.7 ms, p=0.045).

Skeletal muscle glucose uptake was slightly increased by secretin compared to placebo (mean $\pm$ SD secretin vs. placebo, 1.16 ± 0.48 µmol/100g/min vs. 0.77 ± 0.20 µmol/100g/min, p=0.003). Interestingly, this was not associated with MGU after secretin infusions (**Figure 19C.**), whereas BAT GU was (**Figure 19A.**). In contrast, muscle GU and MGU were associated in fasting conditions (**Figure 19D.**).

Serum creatinine decreased briefly after the secretin infusion (**Figure 20A.**), concomitantly with the largest increases of serum secretin levels (**Figure 20C.**). Accordingly, eGFR increased from baseline at thirty minutes after secretin infusion, compared to placebo (**Figure 20B.**). Urine secretion was not significantly changed when assessed for the entire duration of the two-hour scan (mean $\pm$ SD secretin vs. placebo, 152.1 ± 62.3 ml/h vs. 136.2 ± 82.9 ml/h, p=0.467). However, [^{18}F]FDG renal clearance was significantly increased by secretin compared to placebo (**Figure 20D.**) despite increased BAT, myocardial and muscle glucose uptake.

Fatty acid, insulin and glucose levels were also monitored during the scan. Circulating fatty acids were increased for the duration of the PET/CT scan (**Table 2.**). A brief increase in plasma insulin levels was observed, together with a transient, nonsignificant decrease in glucose levels (**Table 2.**).
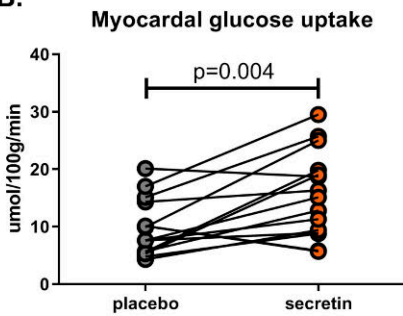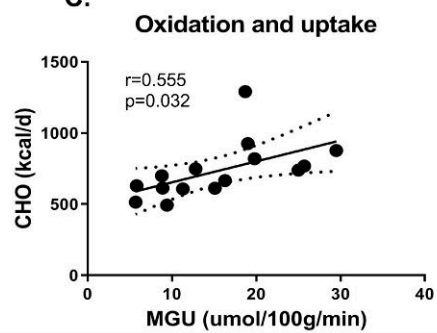
Figure 18. A. Representative PET/CT images of myocardial [^{18}F]FDG uptake after secretin and placebo. (III) **B.** Myocardial glucose uptake (MGU) is increased after secretin compared to placebo. (III) **C.** After secretin infusion, carbohydrate oxidation (CHO) is associated with MGU. (III) Modified from Laurila et al. Manuscript 2021.

A.

Glucose uptake during secretin

r=0.592
p=0.020

B.

Glucose uptake during placebo

r=-0.028
p=0.922

C.

Glucose uptake during secretin

r=0.290
p=0.295

D.

Glucose uptake during placebo

r=0.617
p=0.014
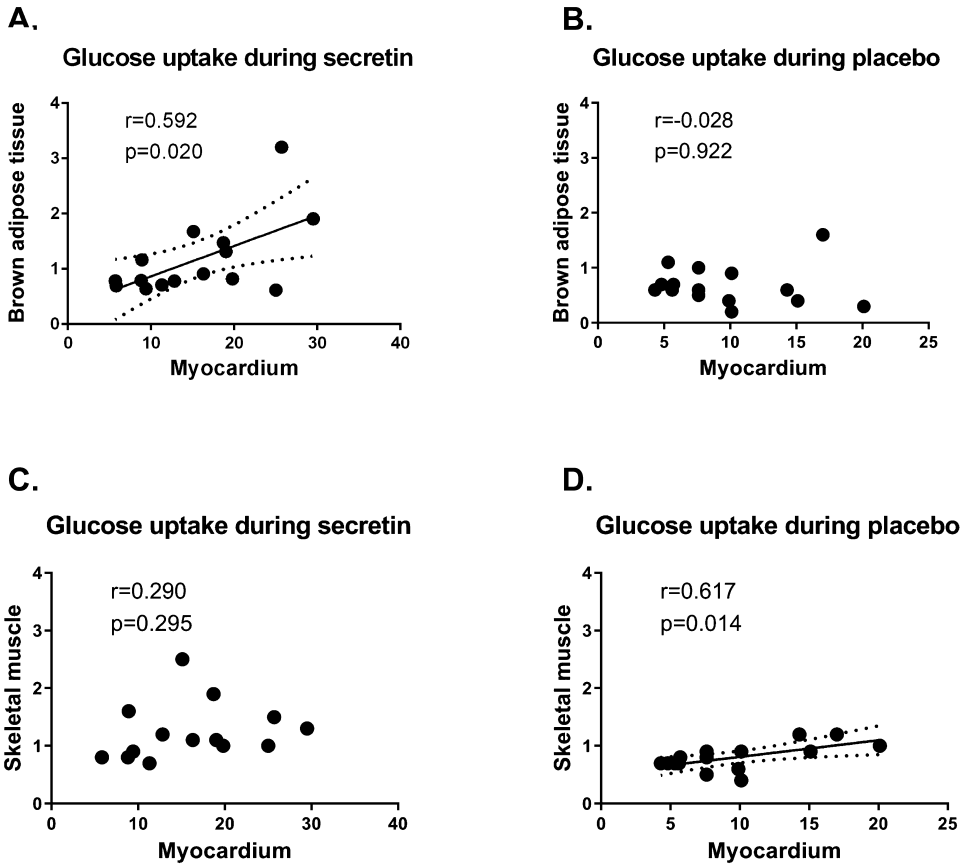
Figure 19. A. Myocardial and brown adipose tissue glucose uptake are strongly associated after secretin infusion, **B.** while this is not the case after placebo. (III) **C.** Myocardial and skeletal muscle glucose uptake are not associated after secretin, **D.** in contrast to after placebo. (III) All glucose uptake units are µmol/100g/min. Modified from Laurila et al Manuscript 2021.
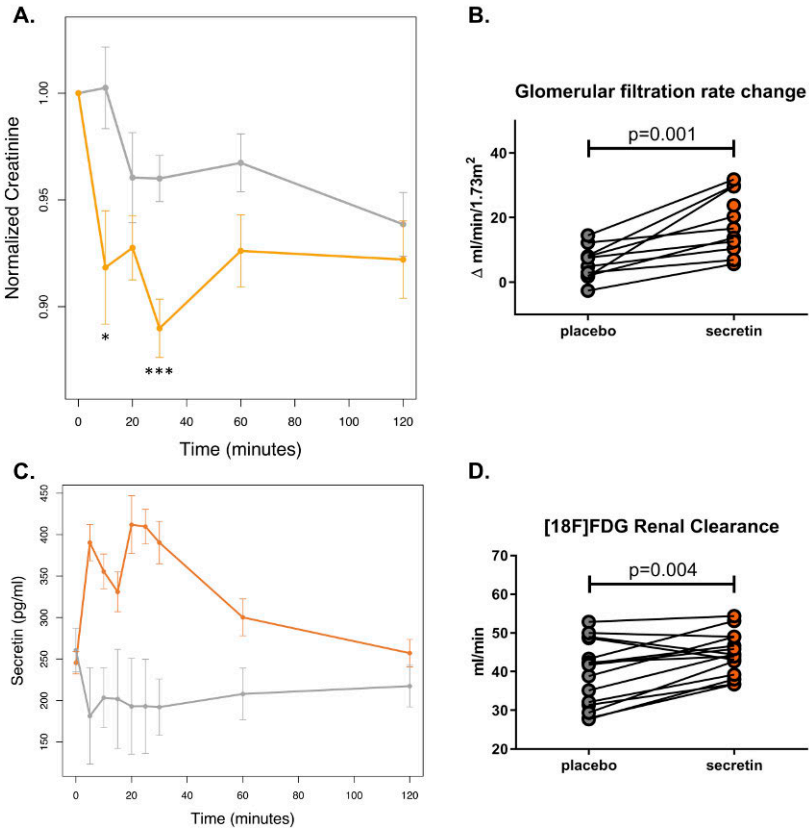
Figure 20. A. Serum creatinine is significantly lower after secretin compared to placebo, directly after infusions given at 0 min and 20 min. (III) **B.** Accordingly, eGFR is increased from baseline at thirty minutes after secretin. (III) **C.** Serum secretin levels peak after infusions given at 0 and 20 minutes. No statistical analysis is included in the image due to only n=4 measured during placebo condition. (II, III) **D.** [18F]FDG renal clearance is increased by secretin compared to placebo, calculated as area under the curve for the duration of the PET/CT scan. (III) Modified from Laurila et al 2021 and Laurila et al. Manuscript 2021.

Table 2. Plasma insulin and glucose, and serum total fatty acids, after secretin and placebo infusions, during the PET/CT scan. Median $\pm$ interquartile range and p value (* p<0.05, ** p<0.01) is shown.

	Time	Secretin	Placebo	p
Insulin (mU/L)	0	6.0 $\pm$ 3.0	7.0 $\pm$ 3.5	
	20	10.0 $\pm$ 9.5	6.0 $\pm$ 3.0	*
	40	5.0 $\pm$ 3.5	5.0 $\pm$ 3.0	
	60	5.0 $\pm$ 2.0	5.0 $\pm$ 4.0	
	120	4.0 $\pm$ 3.0	4.2 $\pm$ 4.0	
Glucose (mmol/l)	0	5.4 $\pm$ 0.3	5.2 $\pm$ 0.5	
	20	5.2 $\pm$ 0.3	5.4 $\pm$ 0.4	
	40	5.3 $\pm$ 0.4	5.3 $\pm$ 0.5	
	60	5.3 $\pm$ 0.4	5.3 $\pm$ 0.3	
	120	5.3 $\pm$ 0.4	5.2 $\pm$ 0.4	
Total Fatty Acids (mmol/l)	0	10.5 $\pm$ 1.3	10.6 $\pm$ 1.4	
	20	10.8 $\pm$ 1.8	10.2 $\pm$ 1.2	**
	30	11.1 $\pm$ 1.7	10.2 $\pm$ 1.3	*
	60	10.9 $\pm$ 1.6	10.1 $\pm$ 1.1	*
	120	10.3 $\pm$ 1.4	10.2 $\pm$ 1.0	

6   Discussion

Obesity is increasing worldwide, and is an independent risk factor for many non-communicable diseases, such as heart disease and cancer (Bessesen and Van Gaal, 2018). In 2017, the global death rate decreased, while the deathrate of non-communicable diseases like cardiovascular disease and neoplasms increased (Roth et al., 2018). Although the globally increasing rate of obesity is not simply a medical question, understanding the physiological mechanisms that influence it is important with regards to prevention and treatment. This thesis presents a new physiological pathway that influences appetite, initiated by the oldest known hormone. Secretin is a pleiotropic hormone and modern era imaging methods have made it possible to study its broad effects in humans *in vivo*.

6.1   Secretin activates BAT in mice and men

This study demonstrates that secretin activates BAT in both mice and healthy, normal weight men, and that secretin has a role in inducing facultative, meal induced thermogenesis. Secretin receptors are abundantly expressed in murine BAT and also present in human BAT. This finding supports a direct action on BAT by the endogenously produced gastric hormone secretin, as well as the secretin analogue used in this study. *In vitro*, non-selective beta blockade attenuated β-AR agonist induced BAT activation, but not secretin induced activation, while in humans, *in vivo* cold induced BAT activation was not associated with secretin induced BAT activation. Since cold induced BAT activation is mediated by the SNS, these results suggest that the effect of secretin on BAT is not mediated by the SNS and supports a direct, hormonal mechanism.

Direct evidence on secretin induced thermogenesis was acquired in mice by studying the temperature of iBAT and the level of oxygenation of venous blood, draining from iBAT. In humans, secretin increased BAT glucose uptake, indicating increased metabolic activity. The dynamic [^{18}F]FDG scan was initiated twenty minutes after the first secretin infusion, simultaneously with the second secretin infusion. Therefore, we were likely able to observe maximal BAT activation during this forty-minute scan.

BAT perfusion is considered an indirect measure of BAT thermogenesis, since BAT perfusion has been shown to associate with BAT oxygen consumption (U-Din et al., 2016). The dynamic radiowater scan was initiated only two minutes after the first secretin infusion and it thus measures an acute BAT perfusion response to intravenous secretin. An increase in BAT perfusion was not observed with the implemented study protocol and it is likely that BAT thermogenesis is initiated at a later time point. In mice, maximal BAT thermogenesis was reached approximately ten minutes after a secretin injection. Since secretin activates BAT in an endogenous manner instead of a more rapid SNS response, optimal timing for measuring BAT perfusion in humans could be at a later timepoint.

Whole body energy expenditure was increased by secretin compared to placebo in both mice and men. This in itself may indicate BAT thermogenesis, but it is likely that other tissues contribute to it as well. Secretin is a pleiotropic hormone and its receptors are present all throughout the body (Chu et al., 2006). Nevertheless, increased energy expenditure shows that secretin could have potential as a catabolic agent.

After mechanistic evidence of BAT activation by secretin was found, secretin's role as a BAT activator during feeding was also investigated. It was shown that feeding increases secretin levels from fasting levels in both mice and men. In mice, these increases were aligned with increases in BAT temperature. In humans, postprandial secretin levels were associated with both BAT fatty acid uptake and oxygen consumption. This shows an association between secretin and meal induced BAT thermogenesis in both rodents and humans.

6.2 Secretin induces satiation in mice and men

It has previously been suggested that facultative meal induced thermogenesis could have a role in regulating energy intake (Glick, 1982; Himms-Hagen, 1995), but this theory has not been fully pursued before. Since secretin is secreted during feeding and it activates BAT, its role on appetite was also investigated in this thesis work. The effect of secretin on appetite has previously only been studied in animals and this thesis work addressed the question in humans for the first time (Chen et al., 2011).

Feeding patterns were investigated in WT and UCP1 KO mice. An intraperitoneal injection of secretin reduced cumulative food intake in WT mice for 2-3 hours, after which there was no difference between the two groups. This is likely due to the short half-life of the commercially available secretin analogues. In humans, the meal size after secretin vs. placebo was only numerically smaller, however the effect size was small for this endpoint (Cohen's d=-0.306).

Interestingly, resumption to refeed was delayed by 39 minutes in humans after secretin compared to placebo.

When meal patterning was investigated in WT and UCP1 KO mice, UCP1 KO mice showed shorter intervals between meals. This could indicate that facultative, meal induced BAT thermogenesis has a role in regulating feeding in mice. The effects of endogenously produced secretin on meal size and patterning were investigated by treating WT mice with a secretin antibody. When secretin's action was blocked, meal size and duration increased compared to controls.

The neurobiological basis of this satiation effect was studied in mice, using biopsy samples from the hypothalamus. Anorexigenic POMC expression increased after secretin injection, while orexigenic AgRP decreased, further supporting the evidence of appetite regulation, already shown with meal patterning. Interestingly, heat sensing capsaicin receptor expression in POMC neurons increased in WT but not UCP1 KO mice after secretin administration. Instead of the previously shown direct endogenous effects of secretin, or those relayed by the ANS to the central nervous system, heat seems to function as a message that leads to the termination of feeding.

The central effects of secretin in humans on appetite was investigated with fMRI and food cue tasks. Remarkably, the reward sensitive coding seen in previous studies (Nummenmaa et al., 2012, 2018) and also here during the placebo scan, was essentially abolished by secretin. Due to technical limitations, it was not possible to study the direct link between BAT thermogenesis and hypothalamic regulation in humans. However, there already exists some indirect evidence of the links between BAT and appetite in humans, as mentioned previously. Mild cold-induced BAT activation is associated with lower serum ghrelin concentrations (Chondronikola et al., 2017) and a thermogenic meal is associated with a sensation of fullness (Crovetti et al., 1998). As to cold induced BAT activation and its association to appetite, one study on healthy males suggests that cold-induced BAT activation is not associated with energy intake or appetite (Sanchez-Delgado et al., 2019). This is in line with the results presented in this thesis work, since the hypothesis is that secretin-induced activation determines energy intake and appetite, rather than cold-induced activation. In our study, secretin not only increased energy expenditure and BAT glucose uptake, but also induced satiation in humans. Thus, this thesis work has come even closer to showing a direct link between BAT activation and appetite suppression.

6.3 Secretin increases myocardial glucose uptake and renal clearance

In recent years, gastric hormones have been of great interest in the field of cardiology. Despite this, secretin has not been studied in humans with modern methods. Almost 40 years ago, Gunnes et al. showed that cardiac output increased significantly during a secretin infusion in patients with heart failure and ischemia (Gunnes and Rasmussen, 1986; Gunnes et al., 1983). The studies were conducted with pulmonary artery catheterization and thermodilution technique, while femoral artery pressure and ECG were also monitored. Systemic resistance fell due to arteriolar dilatation, which has an effect on cardiac output through a decrease in afterload. However, the increase in output was so considerable (20 percent), that an inotropic effect was suggested as well. It could not be proven with the implemented method, but was supported by later findings in animal studies (Bell and McDermott, 1994; Grossini et al., 2013). The increase in MGU with secretin compared to placebo shown in this thesis work supports an inotropic effect by secretin in humans. Fasting [^{18}F]FDG uptake is associated with increased heart work (Duchenne et al., 2019; Masci et al., 2010). Furthermore, there was an association between MGU and carbohydrate oxidation after secretin infusion, which supports the theory that the glucose taken up by the heart is used as an energy substrate.

Another interesting finding was that QTc was shortened after secretin compared to placebo, while there was no difference in heart rate. QTc interval has been shown to shorten postprandially (Taubel et al., 2012) and previous studies indicate that the change is not associated with increased insulin or glucose levels (Taubel et al., 2013). In contrast, high carbohydrate uptake and high insulin levels are associated with a postprandial increase in heart rate, indicating SNS activation (Scott et al., 2002). It has been suggested that postprandial QTc shortening is associated with the signaling pathways of calcium cycling (Täubel et al., 2019). This would be in line with a known postprandial increase in inotropy, also involving calcium cycling (Täubel et al., 2019). As mentioned before; sctr is also G_q-protein coupled, which mobilizes intracellular calcium. Taken together, the QTc shortening seen in this study could be due to increased inotropy. As a prandial hormone, secretin might even influence postprandial QTc shortening and inotropy. Further studies are needed to confirm this.

Secretin activates lipolysis in white adipose tissue (Butcher and Carlson, 1970; Sekar and Chow, 2014) and this study found an increase in serum total FA after secretin compared to placebo. In regards to BAT, this is an interesting finding, since lipolysis is not only important in fueling thermogenesis, but also in its initiation (Blondin et al., 2017). As for the heart, it is notable that glucose uptake increased despite a concomitant increase in circulating FAs. Glucose uptake is regulated

mainly through the recruitment of GLUT4 transporters (Lopaschuk and Stanley, 1997), whereas the rate of FA uptake is mostly determined by arterial FA concentration (An and Rodrigues, 2006). During glucose-insulin clamp conditions, myocardial glucose uptake decreases when FAs are infused (Nuutila et al., 1992). According to our results, secretin increases the availability of FAs as an energy substrate for the heart, yet glucose uptake is still increased. This supports an increase in heart work even further.

As reviewed in this thesis, previous studies have shown somewhat conflicting results on the effect of secretin on fluid homeostasis. When it comes to pathological conditions of the heart and kidneys and their treatments, both are of interest since both conditions exacerbate the other. Effect size was poor for urine secretion measurements in this study (Cohen's d=0.2), but the more accurate measurement of [^{18}F]FDG clearance rate showed increased secretion after secretin compared to placebo. This was complimented by eGFR measurements. The results presented in this thesis suggest a small diuretic effect, but since the rough urine measurements showed no difference between secretin and placebo, the effect is likely too brief or small to affect cardiac output through a decrease in afterload (Wilson et al., 1981). A longer acting secretin analogue could show a more pronounced effect on diuresis.

Interestingly, creatinine clearance rate has previously been shown to associate with BAT activation in humans (Gerngroß et al., 2017). Since eGFR also increases after muscular exercise, this could reflect an increase in creatin phosphate turnover (Refsum and Strömme, 1974). Kazak et al have shown that beige adipose tissue thermogenesis is enhanced by a creatin-driven substrate cycle, which also has a role in diet induced thermogenesis (Kazak et al., 2015, 2017). Taken together, the increase in eGFR shown in this thesis work could also reflect BAT activation.

Glucose uptake was also increased in skeletal muscle by secretin compared to placebo. Interestingly, muscle glucose uptake was associated with MGU after placebo but not secretin, while the opposite occurred with BAT. This could indicate an interaction effect between BAT and the heart, induced by secretin. Secretin is a prandial hormone and cardiac output increases postprandially (Waaler et al., 1991). The exact purpose is not known, but it could be in order to facilitate nutrient distribution and digestion. It could also facilitate the effects that secretin induces in BAT. The interaction might also simply indicate that both effects are similarly regulated through secretin receptors.

6.4   Strengths and limitations

The strength of this study is the implementation of a wide range of methods in both animal models and as proof of concept in healthy male human participants. Mice have a considerably larger BAT mass than humans and when BAT studies are conducted in mouse models, there is always a question of whether the same effect can be found in humans and to which extent. Even if human BAT depots are considerably smaller than those in mice, it is notable that supraclavicular and cervical BAT depots are located close to the carotid arteries. Due to the anatomical localization of human BAT, it has been proposed that thermogenesis protects the normal function of vital organs like the brain in cold exposure (Sacks and Symonds, 2013). Similarly, prandial BAT thermogenesis could relay heat as a message to the central nervous system, despite the small volume of BAT in humans. Of course, the possibility of a direct action of secretin on human appetite in the central nervous system cannot be ruled out by the methods implemented in this thesis work. Future studies are needed to also address whether the results are applicable to other groups than healthy men.

PET/CT is a noninvasive method, but with it, subjects are exposed to ionizing radiation. Administering a 150 MBq dose of [18F]FDG results in a radiation exposure of 2.85 mSv, while 500 MBq dose of [15O]H2O results in 0.55 mSv. This is due to the quicker decay of [15O] compared to [18F]. The radiation exposure of low dose CT for attenuation correction and anatomical localization is minimal, in this study 0.06 mSv for the neck and 0.19 mSv for the chest. The annual background radiation dose in Finland is 3.2 mSv and a two-way transatlantic flight causes a cosmic radiation exposure of around 0.2 mSv. The maximum permitted radiation dose in healthy volunteers is around 10 mSv, corresponding to three years of background radiation.

Since PET tracers are always distributed throughout the whole body, acquiring full body imaging in combination with low dose CT does not significantly increase radiation exposure, while it enables studies to address crosstalk between several organ systems *in vivo*. Currently, the FOV creates a limitation for this. Only a specific body area can be scanned at a time and the size of the FOV depends on the PET scanner. In this study, areas of interest were scanned in succession in order to obtain information on several organs, but this is only possible with tracers that have an adequately long decay time. [18F]FDG is a suitable tracer for this method, while only one area can be scanned with a single injection of [15O]H_2O. In the future, whole body long axial FOV PET scanners will make it possible to quantitatively investigate all organ systems simultaneously. This will make PET an even more impactful tool for investigating organ crosstalk.

PET tracers are always carefully selected based on the study question. Dose, number of tracers and decay time are considered in the planning phase of each study

and this causes some limitations. In this study, fatty acid uptake could not be investigated in combination with [18F]FDG, due to the tracer also being fluoride labeled and having a relatively long decay time. Instead, we conducted a [15O]H2O scan in order to investigate perfusion. Based on the results, it is likely that the timing of the perfusion scan was not timed for maximal BAT activation. Ideally, several [15O]H2O scans could have been conducted in succession, to find the time point for maximal perfusion, but this was not possible within the scope of this study. Also, timing the perfusion scan for maximal BAT activation would have in turn caused limitations to investigating the glucose uptake of other organs, due to the short half-life of secretin hydrochloride.

fMRI is also a noninvasive method, and it does not expose subjects to ionizing radiation. When patients with claustrophobia and those with magnetic implants are excluded, and metal objects are removed before approaching the scanner, MRI is very safe. fMRI is also more objective than traditional questionnaires. However, a common critique in the field is based on what conclusions can really be made based on BOLD signal alone. This issue can be mitigated by implementing previously established protocols. Another critique relates to data analysis. The field has implemented a wide range of modeling and false positives are of concern. This can be limited by increasing sample size and by implementing open code and analysis pipelines. In this study, a previously established food cue method was utilized (Nummenmaa et al., 2012, 2018) in a paired setting and analysis was conducted with fMRIPrep, a pipeline published in Nature Methods (Esteban et al., 2019). Both fMRI and visual analogue scale questions were implemented and provided results that support the hypothesis of secretin having an appetite reducing effect.

As for secretin's effect on caloric intake in humans, further and likely large studies are needed in order to address the question. Our results indicate that a single pre-prandial injection of secretin increases the time before resumption to eat by 39 minutes. Thus, consecutive administration of secretin before each meal could reduce caloric intake. There was also a trend in reduced caloric intake with the first meal after injection, but the sample size was low for investigating this secondary endpoint. Based on our results, if a future study was planned for investigating caloric intake after a single injection of a short acting secretin analogue, sample size is n=78 with power 0.8, significance level 0.05 and effect size of d=-0.306.

Perfusion imaging of the heart would have provided valuable information on cardiac metabolism. This study was planned for investigating BAT activation and the heart could not be fitted into the same FOV as supraclavicular BAT. As to myocardial glucose uptake, patient compliance was good in this study and subjects adhered to instructions on fasting. MGU is very sensitive to changes in circulating glucose levels, and these were not significantly changed by secretin compared to placebo during the [18F]FDG scan.

Urine secretion was only measured with a very rough method in this study. Since secretin hydrochloride has a short half-life, it is likely that the diuretic effect was brief and could not be detected when measured as the secreted urine volume from start to the end of the scan. Urimetry through catheterization would be a more accurate method. [^{18}F]FDG clearance was measured however, which is a more accurate method for measuring renal filtration. The result was also complimented with eGFR measurements. As to renal effects by PET/CT, currently there is no validated way to model cortical glucose uptake with [^{18}F]FDG. Modeling glucose uptake in the kidneys is challenging because of spillover from urine. [^{18}F]FDG is filtrated into urine and unlike glucose, not re-uptaken by sodium-glucose transporter protein 2 (SGLT2), causing significant spillover (Oikonen, n.d.). Unfortunately, renal perfusion could not be measured in this study either, due to the previously mentioned limitations in FOV. In the future, broader organ crosstalk studies could be conducted with long axial PET, ideally with an oxygen tracer in order to investigate tissue oxygen consumption.

6.5   Future aspects

This thesis work addresses the effects of secretin on BAT and appetite in humans for the first time. Taken together, secretin appears to be a compelling pharmacological target for weight management, as it both increases catabolism and reduces motivation to eat. Increased energy expenditure leads to increased energy intake (Polidori et al., 2016), which is why targeting the feedback control of energy intake, instead of only aiming to increase energy expenditure, would be an effective way to treat obesity. A longer acting secretin analogue could provide more pronounced effects than those seen in this study, but it may also be possible that other feedback mechanisms then take effect. Repeated pre-prandial administration of secretin, instead of a very long-acting analogue, could be a possible way to avoid this. Future clinical trials are needed to confirm whether pre-prandially administered secretin has potential in decreasing food intake.

The question of thermogenesis and its effect on appetite still remains unanswered in humans. If not BAT activation, heat itself could be further investigated as a suppressor of appetite. These questions relating to appetite and feeding are especially relevant in insulin resistant and obese subjects, which were not studied in this thesis work. Type 2 diabetes treatments could also have a synergistic effect with secretin. DPP-4 could increase secretin levels in addition to incretins, such as GLP-1 and GIP. The synergy between secretin's effect on appetite and that of the by now well-established appetite suppression of GLP-1 also warrants further studies.

The results of this thesis support that secretin increases heart work and glomerular filtration. The effect of secretin on the heart in pathological conditions like heart failure and type 2 diabetes should be further investigated. With heart failure medications, there could also be synergy with secretin. Sacubitril is a neprilysin inhibitor, which inhibits the breaking down of peptide hormones, most clinically significantly natriuretic peptide. However, studies have also shown improved glycemic control in diabetic heart failure patients, likely due to neprilysin's inhibition on the breaking down of incretins (Seferovic et al., 2017). This could also be the case with secretin.

7   Conclusions

This thesis aimed to investigate the potential of secretin as an activator of facultative, meal induced BAT thermogenesis (Study I and II) and its influence on appetite (Study I and II). Since secretin is considered a pleiotropic hormone, the broad effects of secretin hydrochloride on metabolism and organ crosstalk were also investigated further (Study II and III). The main findings of the studies were the following:

1. Secretin receptors were shown in human BAT by immunohistochemistry. Compared to placebo, secretin increased glucose uptake in human BAT and whole-body energy expenditure, measured by indirect calorimetry. Postprandial serum secretin levels were associated with BAT oxygen and fatty acid uptake.

2. Appetite was reduced by secretin compared to placebo when measured with composite satiety score and an fMRI food cue task. Resumption to eat was increased after secretin compared to placebo.

3. Secretin increased myocardial glucose uptake compared to placebo. This was associated with carbohydrate oxidation. QTc was shortened after secretin compared to placebo, while heart rate was not changed. Skeletal muscle glucose uptake, renal filtration and circulating fatty acids also increased after secretin compared to placebo.

In summary, this thesis shows that secretin not only has potential as a catabolic agent through BAT activation, but also plays a role in the control of food intake. This novel link between thermogenesis and satiation opens up new avenues for obesity research. The results also support an inotropic effect on the heart, which has been suggested in previous studies. Secretin also increases renal filtration. These two effects warrant further studies in relation to heart failure, as both could be beneficial.

Acknowledgements

I wish to sincerely thank my supervisors Professor Pirjo Nuutila and Docent Kirsi Virtanen for the opportunity to conduct my doctoral thesis under their guidance. Pirjo, your enthusiasm for research and skills as a clinician are inspiring. You have more hours in your day than most, especially for those you supervise. Kirsi, your positivity, devotion to research and expertise on BAT are beyond compare. You two have built a scientifically formidable group with a lot of heart, who welcomed me with open arms and helped me start this project. Pirjo and Kirsi, I thank you for seeing potential in me and giving me so much responsibility in this project. I can always count on your support and brilliant advice.

I express my gratitude to the reviewers of this thesis, Adjunct Professor Kirsi Timonen and Docent Tiinamaija Tuomi. Your observations and perspectives improved this work considerably. I would also like to thank Professor Kirsi Pietiläinen for being a member of my PhD follow-up committee. I am grateful to Professor Francesc Villarroya for accepting the invitation to act as my opponent in the dissertation defence and I look forward to our discussions.

I wish to thank all my collaborators and co-authors who have played a key role in the work presented in this thesis. Professor Martin Klingenspor, your knowledge and vision is astounding. I am honoured and privileged for having had this chance to work with you. Katharina Schnabl, you are a brilliant scientist with excellent ideas. I look forward to working with you in the future. I am very grateful to the excellent biopsy team Tarja Niemi and Markku Taittonen for providing their valuable expertise in obtaining the human brown adipose tissue samples, and Katja Steiger, for providing her expertise as a skilled and experienced pathologist. Professor Lauri

Nummenmaa, thank you for providing your expertise on imaging reward responses. I am also extremely grateful that you coached me through the statistics comments of Reviewer 2, who proved a formidable final boss. I also want to thank Adjunct Professor Kirsi Laitinen for her expertise on nutrition and appetite. Adjunct Professor Riku Klén, thank you for the effortless co-operation. You are amazingly quick and precise.

I wish to thank Minna, Mia and Lihua, whose commitment to imaging studies made this work possible. Minna Lahesmaa, you are highly experienced in BAT physiology, as well as conducting studies and analysis. You taught me and helped me get started, while also making me feel welcome from the moment we met. Working with you was an absolute joy and I am grateful for gaining a lifelong friend in you. Thank you, Mia Koutu, for coordinating the study whenever I could not and in the beginning teaching me the practicalities. You are a quick thinker and problem solver, efficient at multitasking and have a high sense of research ethics. You also always prioritize the wellbeing of study volunteers and make them feel safe and cared for, which is extremely important for a study nurse. Lihua Sun, for extremely fruitful and pleasant collaborations. You are always eager to test new hypotheses and thanks to your commitment, we were able to not only study BAT physiology, but also the crosstalk between BAT and brain. You are not only brilliant, but also extremely hard working. I can always count on you coming through. I will always remember the weekends at the end of 2017, when the four of us worked like well-oiled machinery and laughed at how nuts we were for spending Christmas scanning volunteers and serving them heaps of casserole. Lastly, Minna and Mia, I hope I was able to convey how much I valued your hard work and help during this project, because I am beyond grateful for the way you two stepped in, especially in the fall of 2016 when family matters demanded my full attention.

I want to also thank the volunteers for committing to this study, even after enduring 4 hours of "mild" cold exposure. Thank you especially to those of you who kept agreeing to come back, when I called to recruit you for yet another part of the study. You were all extremely committed and patient, and all of this would have been impossible without you.

I would also like to thank Aino Latva-Rasku, for teaching me the ropes in the beginning. You are efficient and precise, both when it comes to adhering to protocol during studies and planning them. Learning this precision was vital when I planned my own PhD project. Thank you also for the fun congress trips and discussions during lunch, you have an excellent sense of humour. Mueez U-Din, thank you for your expertise in BAT physiology and analysis. You taught me a lot of important methods and working with you has been wonderful. I would also like to thank the brilliant Eleni Rebelos, whom I have enjoyed working with immensely. You are a powerhouse of ideas and persistent in pursuing results. Working with you has been

inspiring and full of laughter. Miikka Honka, you've been an important presence at the PET Centre from the very beginning and we have had a lot of fun both at and outside of work. You are also a knowledge bank, remembering all methods, projects and researchers that came and left the PET Centre. Prince Dadson, for welcoming me into the downstairs community. Sharing a booth with you was a wonderful time and I wonder how you managed to be so extremely productive, when the whole centre always walked past you and staid to chat. You helped me with a lot of practical issues in the beginning and debating politics was a good counterbalance to work.

I wish to also thank many, many others at the PET Centre. The physicists Kalle Koskensalo, Jukka Ihalainen and Madoka Ogawa for fruitful collaboration, and Mika Teräs, Virva Saunavaara, Tuula Tolvanen and Jarmo Teuho for their expertise. The entire laboratory staff and especially Sanna Suominen for all her advice and knowledge. Also the radiographers, especially Minna Aatsinki for her patience and help with creatively timed scanning slots. The whole staff upstairs, you are professional and extremely fun to work with and I look forward to working with you all in the future! Docents Jarna Hannukainen and Marco Bucci, for their help and encouragement in the beginning. Sanna Himanen, for your positive attitude and help. I look forward to continuing our work! Fellow investigators Laura Pekkarinen, Tatu Kantonen, Sanna Honkala, Marja Heiskanen, Ronja Ojanen, Priyanka Motiani, Kumail Motiani, Tanja Sjöros, Eduardo Juárez-Orozco, Juho Raiko, Teemu Saari, Jukka Koffert, Henry Karlsson, Olli Moisio, Tia-Mari Peltomaa, Francisco Acosta, Teemu Maaniitty, Milena Monfort Pires, Tuulia Malén, Jouni Tuisku, Janne Isojärvi, Laura Ekblad, Sini Toppala, Anniina Snellman, Petri Elo, Janne Verho and Heidi Immonen. Thank you for the collaborations, lunches, congress trips, conversations, ideas and fun karonkka parties. Special thanks to team "Ydinryhmä" or "Miikka plus five": Eleni, Minna, Miikka, Riikka Siitonen, Mia Ståhle, Simona Malaspina and Kerttu Seppälä. Be it card games, sports, food and wine or beach outings, we always have a fun time and I am extremely grateful to have you in my life.

I also want to thank all my superiors in the clinics during this project for granting me time off for research: Marjatta Strandberg, Jan Sundell, Heikki Ukkonen, Pirjo Rummukainen and Riikka Lautamäki. The way you see value in science made this work possible. Pirjo and Juha Rummukainen, thank you for your endless support and positivity. Heikki and Riikka, you are both excellent role models and I am fortunate to work with you. I also want to thank Professors Juhani Airaksinen and Antti Saraste, your enthusiasm for cardiology, research and teaching is inspiring. Thank you for your guidance.

I also want to thank my friends outside of science, for providing me with the work-life balance that made this journey possible. Thank you for making me laugh and being my cornerstones throughout the years. Spending time with you recharges my mind. Minttu and Riina, you've been an important part of my life ever since we

were kids. Arf and the extended arflings: Jutta, Joe, Linda, Petter, Natasha, Anna R., Stefan, Anna S., Bogdan, Jusu, Yoojin, Maxine and Shereif, for being my family of nerds since the early Turku years, providing support, fun and honing my English. The inspiring superwomen: Elina, Säde and Maija, for stimulating discussions and encouragement. Pyry, Maija and Anna for bringing laughter and music to my evenings. Maaria, for wine, discussions, choir and nights out in town. Johanna and Meeri, for always cheering me up. Sofia, Heljä and Joonas, for the joy and support you've given me. My fellow specializing internists and cardiologists throughout this journey, for peer support and fun.

Lastly, I wish to thank my family. Seija, I see you in the eyes of my siblings. Thank you for giving us more than any child could hope for. As I said in 2016: don't worry, we will be alright. Jouni, thank you for encouraging my curiosity in science. You have always supported me in my work and cheered me on. My brother Matti and my sister Anni for your support and the joy you give me. Finally, I wish to thank Juha, whose support I have always been able to count on. Thank you for being my home through this journey.

30.5.2021
Sanna Laurila

References

Afroze, S., Meng, F., Jensen, K., McDaniel, K., Rahal, K., Onori, P., Gaudio, E., Alpini, G., and Glaser, S.S. (2013). The physiological roles of secretin and its receptor. Ann. Transl. Med. 1, 29.

Aherne, W., and Hull, D. (1966). Brown adipose tissue and heat production in the newborn infant. J. Pathol. Bacteriol. 91, 223–234.

An, D., and Rodrigues, B. (2006). Role of changes in cardiac metabolism in development of diabetic cardiomyopathy. Am. J. Physiol. - Hear. Circ. Physiol. 291.

Anand, S.S., Singh, H., and Dash, A.K. (2009). Clinical applications of PET and PET-CT. Med. J. Armed Forces India 65, 353–358.

Astrup, A., Rössner, S., Van Gaal, L., Rissanen, A., Niskanen, L., Al Hakim, M., Madsen, J., Rasmussen, M.F., and Lean, M.E. (2009). Effects of liraglutide in the treatment of obesity: a randomised, double-blind, placebo-controlled study. Lancet 374, 1606–1616.

Avants, B.B., Epstein, C.L., Grossman, M., and Gee, J.C. (2008). Symmetric diffeomorphic image registration with cross-correlation: Evaluating automated labeling of elderly and neurodegenerative brain. Med. Image Anal.

Babkin, B.P. (1949). Pavlov, a Biography. (Chicago: University of Chicago Press).

Babu, G.N., and Vijayan, E. (1983). Plasma gonadotropin, prolactin levels and hypothalamic tyrosine hydroxylase activity following intraventricular bombesin and secretin in ovariectomized conscious rats. Brain Res. Bull. 11, 25–29.

Bachman, E.S., Dhillon, H., Zhang, C.Y., Cinti, S., Bianco, A.C., Kobilka, B.K., and Lowell, B.B. (2002). βAR signaling required for diet-induced thermogenesis and obesity resistance. Science (80-.). 297, 843–845.

Banks, W.A., Goulet, M., Rusche, J.R., Niehoff, M.L., and Boismenu, R. (2002). Differential transport of a secretin analog across the blood-brain and blood-cerebrospinal fluid barriers of the mouse. J. Pharmacol. Exp. Ther. 302, 1062–1069.

Barbezat, G.O., Isenberg, J.I., and Grossman, M.I. (1972). Diuretic Action of Secretin in Dog. Proc. Soc. Exp. Biol. Med. 139, 211–215.

Bauman, M.L. (1991). Microscopic neuroanatomic abnormalities in autism. Pediatrics 87, 791–796.

Bayliss, W.M., and Starling, E.H. (1902). The mechanism of pancreatic secretion. J. Physiol. 28, 325–353.

Bazzett, H. (1920). An analysis of the time-relations of electrocardiograms. Heart 7, 353–37.

Becher, T., Palanisamy, S., Kramer, D.J., Eljalby, M., Marx, S.J., Wibmer, A.G., Butler, S.D., Jiang, C.S., Vaughan, R., Schöder, H., et al. (2021). Brown adipose tissue is associated with cardiometabolic health. Nat. Med. 27, 58–65.

Behzadi, Y., Restom, K., Liau, J., and Liu, T.T. (2007). A component based noise correction method (CompCor) for BOLD and perfusion based fMRI. Neuroimage.

Beiroa, D., Imbernon, M., Gallego, R., Senra, A., Herranz, D., Villarroya, F., Serrano, M., Fernø, J., Salvador, J., Escalada, J., et al. (2014). GLP-1 agonism stimulates brown adipose tissue thermogenesis and browning through hypothalamic AMPK. Diabetes 63, 3346–3358.

Bell, D., and McDermott, B.J. (1994). Secretin and vasoactive intestinal peptide are potent stimulants of cellular contraction and accumulation of cyclic AMP in rat ventricular cardiomyocytes. J. Cardiovasc. Pharmacol. 23, 959–969.

Bell, P.M., Henry, R.W., Buchanan, K.D., and Alberti, K.G.M.M. (1985). Cimetidine fails to suppress the rise in plasma secretin during fasting. Regul. Pept. 10, 127–131.

Bessesen, D.H., and Van Gaal, L.F. (2018). Progress and challenges in anti-obesity pharmacotherapy. Lancet Diabetes Endocrinol. 6, 237–248.

Blondin, D.P., Labbé, S.M., Tingelstad, H.C., Noll, C., Kunach, M., Phoenix, S., Guérin, B., Turcotte, Eric E., Carpentier, A.C., Richard, D., et al. (2014). Increased brown adipose tissue oxidative capacity in cold-acclimated humans. J. Clin. Endocrinol. Metab. 99.

Blondin, D.P., Frisch, F., Phoenix, S., Guérin, B., Turcotte, É.E., Haman, F., Richard, D., and Carpentier, A.C. (2017). Inhibition of Intracellular Triglyceride Lipolysis Suppresses Cold-Induced Brown Adipose Tissue Metabolism and Increases Shivering in Humans. Cell Metab. 25.

Blouet, C., and Schwartz, G.J. (2012). Duodenal Lipid Sensing Activates Vagal Afferents to Regulate Non-Shivering Brown Fat Thermogenesis in Rats. PLoS One 7, e51898.

Bodanszky, M., Ondetti, M.A., Levine, S.D., and Williams, N.J. (1967). Synthesis of Secretin. II. The Stepwise Approach. J. Am. Chem. Soc. 89, 6753–6757.

Bøtker, H.E., Böttcher, M., Schmitz, O., Gee, A., Hansen, S.B., Cold, G.E., Nielsen, T.T., and Gjedde, A. (1997). Glucose uptake and lumped constant variability in normal human hearts determined with [18F]fluorodeoxyglucose. J. Nucl. Cardiol. Off. Publ. Am. Soc. Nucl. Cardiol. 4, 125–132.

Braun, K., Oeckl, J., Westermeier, J., Li, Y., and Klingenspor, M. (2018). Non-adrenergic control of lipolysis and thermogenesis in adipose tissues. J. Exp. Biol. 121.

Broeders, E.P.M., Nascimento, E.B.M., Havekes, B., Brans, B., Roumans, K.H.M., Tailleux, A., Schaart, G., Kouach, M., Charton, J., Deprez, B., et al. (2015). The Bile Acid Chenodeoxycholic Acid Increases Human Brown Adipose Tissue Activity. Cell Metab. 22, 418–426.

Butcher, R.W., and Carlson, L.A. (1970). Effects of secretin on fat mobilizing lipolysis and cyclic AMP levels in rat adipose tissue. Acta Physiol. Scand. 79, 559–563.

Buxton, R.B., Uludağ, K., Dubowitz, D.J., and Liu, T.T. (2004). Modeling the hemodynamic response to brain activation. In NeuroImage, (Academic Press), pp. S220–S233.

Cannon, B., and Nedergaard, J. (2004). Brown Adipose Tissue: Function and Physiological Significance. Physiol. Rev. 84, 277–359.

Carpentier, A.C., Blondin, D.P., Virtanen, K.A., Richard, D., Haman, F., and Turcotte, É.E. (2018). Brown Adipose Tissue Energy Metabolism in Humans. Front. Endocrinol. (Lausanne). 9.

Chamokova, B., Bastati, N., Poetter-Lang, S., Bican, Y., Hodge, J.C., Schindl, M., Matos, C., and Ba-Ssalamah, A. (2018). The clinical value of secretin-enhanced MrcP in the functional and morphological assessment of pancreatic diseases. Br. J. Radiol. 91.

Charlton, C.G., Quirion, R., Handelmann, G.E., Miller, R.L., Jensen, R.T., Finkel, M.S., and O'Donohue, T.L. (1986). Secretin receptors in the rat kidney: Adenylate cyclase activation and renal effects. Peptides 7, 865–871.

Chen, C.Y.Y., Chu, J.Y.S., and Chow, B.K.C. (2011). Central and Peripheral Administration of Secretin Inhibits Food Intake in Mice through the Activation of the Melanocortin System. Neuropsychopharmacology 36178, 459–471.

Cherry, S.R., and Dahlbom, M. (2006). PET: Physics, Instrumentation, and Scanners (Springer New York).

Chey, W.Y., and Chang, T.M. (2003). Secretin, 100 years later. J. Gastroenterol. 38, 1025–1035.

Chey, W.Y., and Chang, T.M. (2014). Secretin: Historical perspective and current status. Pancreas 43, 162–182.

Chey, W.Y., Lee, Y.H., Hendricks, J.G., Rhodes, R.A., and Tai, H.H. (1978). Plasma secretin concentrations in fasting and postprandial state in man. Am. J. Dig. Dis. 23, 981–988.

Chey, W.Y., Kim, M.S., Lee, K.Y., and Chang, T.M. (1979). Effect of rabbit antisecretin serum on postprandial pancreatic secretion in dogs. Gastroenterology 77, 1268–1275.

Chondronikola, M., Volpi, E., Børsheim, E., Porter, C., Annamalai, P., Enerbäck, S., Lidell, M.E., Saraf, M.K., Labbe, S.M., Hurren, N.M., et al. (2014). Brown adipose tissue improves whole-body glucose homeostasis and insulin sensitivity in humans. Diabetes 63.

Chondronikola, M., Porter, C., Malagaris, I., Nella, A.A., and Sidossis, L.S. (2017). Brown adipose tissue is associated with systemic concentrations of peptides secreted from the gastrointestinal system and involved in appetite regulation. Eur. J. Endocrinol. 177, 33–40.

Chu, J.Y.S., Yung, W.H., and Chow, B.K.C. (2006). Secretin: A pleiotrophic hormone. In Annals of the New York Academy of Sciences, (Blackwell Publishing Inc.), pp. 27–50.

Chu, J.Y.S., Chung, S.K.S.C.K., Lam, A.K.M., Tam, S., Chung, S.K.S.C.K., and Chow, B.K.C. (2007). Phenotypes developed in secretin receptor-null mice indicated a role for secretin in regulating renal water reabsorption. Mol. Cell. Biol. 27, 2499–2511.

Chu, J.Y.S., Lee, L.T.O., Lai, C.H., Vaudry, H., Chan, Y.S., Yung, W.H., and Chow, B.K.C. (2009). Secretin as a neurohypophysial factor regulating body water homeostasis. Proc. Natl. Acad. Sci. U. S. A. 106, 15961–15966.

Chu, J.Y.S., Cheng, C.Y.Y., Lee, V.H.Y., Chan, Y., and Chow, B.K.C. (2011). Secretin and body fluid homeostasis. Kidney Int. 79397, 280–287.

Chu, J.Y.S., Cheng, C.Y.Y., Sekar, R., and Chow, B.K.C. (2013). Vagal Afferent Mediates the Anorectic Effect of Peripheral Secretin. PLoS One 8, e64859.

Clark Mason, J., Murphy, R.F., Welby Henry, R., and Buchanan, K.D. (1979). Starvation-induced changes in secretin-like immunoreactivity of human plasma. BBA - Gen. Subj. 582, 322–331.

Cockcroft, D.W., and Gault, M.H. (1976). Prediction of creatinine clearance from serum creatinine. Nephron 16, 31–41.

CONSESUS (1987). Effects of Enalapril on Mortality in Severe Congestive Heart Failure. N. Engl. J. Med. 316, 1429–1435.

Cosentino, F., Grant, P.J., Aboyans, V., Bailey, C.J., Ceriello, A., Delgado, V., Federici, M., Filippatos, G., Grobbee, D.E., Hansen, T.B., et al. (2020). 2019 ESC Guidelines on diabetes, pre-diabetes, and cardiovascular diseases developed in collaboration with the EASD. Eur. Heart J. 41, 255–323.

Cox, R.W. (1996). AFNI: Software for analysis and visualization of functional magnetic resonance neuroimages. Comput. Biomed. Res.

Crovetti, R., Porrini, M., Santangelo, A., and Testolin, G. (1998). The influence of thermic effect of food on satiety. Eur. J. Clin. Nutr. 52, 482–488.

Cypess, A.M., Lehman, S., Williams, G., Tal, I., Rodman, D., Goldfine, A.B., Kuo, F.C., Palmer, E.L., Tseng, Y.-H., Doria, A., et al. (2009). Identification and importance of brown adipose tissue in adult humans. N. Engl. J. Med. 360, 1509–1517.

Cypess, A.M., Haft, C.R., Laughlin, M.R., and Hu, H.H. (2014). Brown fat in humans: Consensus points and experimental guidelines. Cell Metab. 20, 408–415.

Dale, A.M., Fischl, B., and Sereno, M.I. (1999). Cortical surface-based analysis: I. Segmentation and surface reconstruction. Neuroimage.

Danad, I., Uusitalo, V., Kero, T., Saraste, A., Raijmakers, P.G., Lammertsma, A.A., Heymans, M.W., Kajander, S.A., Pietilä, M., James, S., et al. (2014). Quantitative assessment of myocardial perfusion in the detection of significant coronary artery disease: Cutoff values and diagnostic accuracy of quantitative [15O]H2O PET imaging. J. Am. Coll. Cardiol. 64, 1464–1475.

Dong, M., and Miller, L.J. (2002). Molecular pharmacology of the secretin receptor. Receptors Channels 8, 189–200.

Dreiling, D.A. (1975). Pancreatic secretory testing in 1974. Gut 16, 653–657.

Duchenne, J., Turco, A., Ünlü, S., Pagourelias, E.D., Vunckx, K., Degtiarova, G., Bézy, S., Cvijic, M., Nuyts, J., Claus, P., et al. (2019). Left Ventricular Remodeling Results in Homogenization of Myocardial Work Distribution. Circ. Arrhythm. Electrophysiol. 12, e007224.

Esteban, O., Markiewicz, C.J., Blair, R.W., Moodie, C.A., Isik, A.I., Erramuzpe, A., Kent, J.D., Goncalves, M., DuPre, E., Snyder, M., et al. (2019). fMRIPrep: a robust preprocessing pipeline for functional MRI. Nat. Methods.

Flint, A., Raben, A., Blundell, J.E., and Astrup, A. (2000). Reproducibility, power and validity of visual analogue scales in assessment of appetite sensations in single test meal studies. Int. J. Obes. Relat. Metab. Disord. 24, 38–48.

Fonov, V., Evans, A., McKinstry, R., Almli, C., and Collins, D. (2009). Unbiased nonlinear average age-appropriate brain templates from birth to adulthood. Neuroimage.

Garcia, G.L., Dong, M., and Miller, L.J. (2012). Differential determinants for coupling of distinct G proteins with the class B secretin receptor. Am. J. Physiol. - Cell Physiol. 302, C1202.

Gardner, J.D., and Jensen, R.T. (1981). Regulation of pancreatic enzyme secretion in vitro. Physiol. Gastrointest. Tract. New York Raven Press 2, 831–837.

Gerngroß, C., Schretter, J., Klingenspor, M., Schwaiger, M., and Fromme, T. (2017). Active Brown Fat During 18F-FDG PET/CT Imaging Defines a Patient Group with Characteristic Traits and an Increased Probability of Brown Fat Redetection. J. Nucl. Med. 58, 1104–1110.

Gilbert, J.-A., Gasteyger, C., Raben, A., Meier, D.H., Astrup, A., and Sjödin, A. (2012). The Effect of Tesofensine on Appetite Sensations. Obesity 20, 553–561.

Glick, Z. (1982). Inverse relationship between brown fat thermogenesis and meal size: the thermostatic control of food intake revisited. Physiol. Behav. 29, 1137–1140.

Glick, Z., Teague, R.J., and Bray, G.A. (1981). Brown adipose tissue: thermic response increased by a single low protein, high carbohydrate meal. Science 213, 1125–1127.

Gorgolewski, K., Burns, C.D., Madison, C., Clark, D., Halchenko, Y.O., Waskom, M.L., and Ghosh, S.S. (2011). Nipype: A flexible, lightweight and extensible neuroimaging data processing framework in Python. Front. Neuroinform.

Greve, D.N., and Fischl, B. (2009). Accurate and robust brain image alignment using boundary-based registration. Neuroimage.

Grossini, E., Molinari, C., Morsanuto, V., Mary, D.A.S.G., and Vacca, G. (2013). Intracoronary secretin increases cardiac perfusion and function in anaesthetized pigs through pathways involving β-adrenoceptors and nitric oxide. Exp. Physiol. 98, 973–987.

Gunnes, P., and Rasmussen, K. (1986). Haemodynamic effects of pharmacological doses of secretin in patients with impaired left ventricular function. Eur. Heart J. 7, 146–149.

Gunnes, P., Waldum, H.L., Rasmussen, K., Ostensen, H., and Burhol, P.G. (1983). Cardiovascular effects of secretin infusion in man. Scand. J. Clin. Lab. Invest. 43, 637–642.

Häcki, W.H. (1980). Secretin. Clin. Gastroenterol. 9, 609–632.

Hanssen, M.J.W., Hoeks, J., Brans, B., van der Lans, A.A.J.J., Schaart, G., van den Driessche, J.J., Jörgensen, J.A., Boekschoten, M. V, Hesselink, M.K.C., Havekes, B., et al. (2015). Short-term cold acclimation improves insulin sensitivity in patients with type 2 diabetes mellitus. Nat. Med. 21.

Heaton, J.M. (1972). The distribution of brown adipose tissue in the human. J. Anat. 112, 35–39.

Himms-Hagen, J. (1995). Role of brown adipose tissue thermogenesis in control of thermoregulatory feeding in rats: a new hypothesis that links thermostatic and glucostatic hypotheses for control of food intake. Proc. Soc. Exp. Biol. Med. 208, 159–169.

Horvath, K., Stefanatos, G., Sokolski, K.N., Wachtel, R., Nabors, L., and Tildon, J.T. (1998). Improved social and language skills after secretin administration in patients with autistic spectrum disorders. J. Assoc. Acad. Minor. Phys. 9, 9–15.

Huettel, S.A., Song, A.W., and Mccarthy, G. (2004). FUNCTIONAL Magnetic Resonance Imaging SECOND EDITION.

Huttunen, P., Hirvonen, J., and Kinnula, V. (1981). The occurrence of brown adipose tissue in outdoor workers. Eur. J. Appl. Physiol. Occup. Physiol. 46, 339–345.

Ikeda, K., Maretich, P., and Kajimura, S. (2018). The Common and Distinct Features of Brown and Beige Adipocytes. Trends Endocrinol. Metab. 29, 191–200.

Ip, N.Y., Baldwin, C., and Zigmond, R.E. (1985). Regulation of the concentration of adenosine 3',5'-cyclic monophosphate and the activity of tyrosine hydroxylase in the rat superior cervical ganglion by three neuropeptides of the secretin family. J. Neurosci. 5, 1947–1954.

Jakus, P.B., Sandor, A., Janaky, T., and Farkas, V. (2008). Cooperation between BAT and WAT of rats in thermogenesis in response to cold, and the mechanism of glycogen accumulation in BAT during reacclimation. J. Lipid Res. 49, 332–339.

Jenkinson, M., Bannister, P., Brady, M., and Smith, S. (2002). Improved optimization for the robust and accurate linear registration and motion correction of brain images. Neuroimage.

Jorpes, E., and Mutt, V. (1961). On the Biological Activity and Amino Acid Composition of Secretin. Acta Chem. Scand. 15, 1790–1791.

Jukkola, P.I., Rogers, J.T., Kaspar, B.K., Weeber, E.J., and Nishijima, I. (2011). Secretin deficiency causes impairment in survival of neural progenitor cells in mice. Hum. Mol. Genet. 20, 1000–1007.

Kalinovich, A. V., de Jong, J.M.A., Cannon, B., and Nedergaard, J. (2017). UCP1 in adipose tissues: two steps to full browning. Biochimie 134.

Kazak, L., Chouchani, E.T., Jedrychowski, M.P., Erickson, B.K., Shinoda, K., Cohen, P., Vetrivelan, R., Lu, G.Z., Laznik-Bogoslavski, D., Hasenfuss, S.C., et al. (2015). A Creatine-Driven Substrate Cycle Enhances Energy Expenditure and Thermogenesis in Beige Fat. Cell 163, 643–655.

Kazak, L., Chouchani, E.T., Lu, G.Z., Jedrychowski, M.P., Bare, C.J., Mina, A.I., Kumari, M., Zhang, S., Vuckovic, I., Laznik-Bogoslavski, D., et al. (2017). Genetic Depletion of Adipocyte Creatine Metabolism Inhibits Diet-Induced Thermogenesis and Drives Obesity. Cell Metab.

Kim, K., Huang, S., Fletcher, L.A., O'Mara, A.E., Tal, I., Brychta, R.J., Cypess, A.M., Chen, K.Y., and Leitner, B.P. (2019). Whole Body and Regional Quantification of Active Human Brown Adipose Tissue Using <sup>18</sup>F-FDG PET/CT. J. Vis. Exp. e58469.

Kim, M.S., Lee, K.Y., and Chey, W.Y. (1979). Plasma secretin concentrations in fasting and postprandial states in dog. Am. J. Physiol. Endocrinol. Metab. Gastrointest. Physiol. 5.

Klein, A., Ghosh, S.S., Bao, F.S., Giard, J., Häme, Y., Stavsky, E., Lee, N., Rossa, B., Reuter, M., Chaibub Neto, E., et al. (2017). Mindboggling morphometry of human brains. PLoS Comput. Biol.

Kooijman, S., van den Heuvel, J.K., and Rensen, P.C.N. (2015). Neuronal Control of Brown Fat Activity. Trends Endocrinol. Metab. 26, 657–668.

Köves, K., Kausz, M., Reser, D., Illyés, G., Takács, J., Heinzlmann, A., Gyenge, E., and Horváth, K. (2004). Secretin and autism: A basic morphological study about the distribution of secretin in the nervous system. Regul. Pept. 123, 209–216.

Kozak, L.P. (2010). Brown Fat and the Myth of Diet-Induced Thermogenesis. Cell Metab. 11, 263–267.

Krishnaswami, S. (2011). A Systematic Review of Secretin for Children With Autism Spectrum Disorders . Pediatr. .

Lahesmaa, M., Oikonen, V., Helin, S., Luoto, P., U-Din, M., Pfeifer, A., Nuutila, P., and Virtanen, K.A. (2019). Regulation of human brown adipose tissue by adenosine and A2A receptors – studies with [15O]H2O and [11C]TMSX PET/CT. Eur. J. Nucl. Med. Mol. Imaging 46, 743–750.

Lameire, N., Vanholder, R., Ringoir, S., and Leusen, I. (1980). Role of Medullary Hemodynamics in the Natriuresis of Drug-Induced Renal Vasodilation in the Rat. Circ. Res. 47, 839–844.

van der Lans, A.A.J.J., Hoeks, J., Brans, B., Vijgen, G.H.E.J., Visser, M.G.W., Vosselman, M.J., Hansen, J., Jörgensen, J.A., Wu, J., Mottaghy, F.M., et al. (2013). Cold acclimation recruits human brown fat and increases nonshivering thermogenesis. J. Clin. Invest. 123, 3395–3403.

Latva-Rasku, A., Honka, M.J., Kullberg, J., Mononen, N., Lehtimäki, T., Saltevo, J., Kirjavainen, A.K., Saunavaara, V., Iozzo, P., Johansson, L., et al. (2019). The SGLT2 inhibitor dapagliflozin reduces liver fat but does not affect tissue insulin sensitivity: A randomized, double-blind, placebo-controlled study with 8-week treatment in type 2 diabetes patients. In Diabetes Care, (American Diabetes Association Inc.), pp. 931–937.

Laurila, S., Lahesmaa, M., Nuutila, P., and Virtanen, K.A. (2020). Ruskean rasvakudoksen toiminta ja merkitys. Duodecim. 136, 625–632.

Lee, S.M.Y., Chen, L., Chow, B.K.C., and Yung, W.H. (2005). Endogenous release and multiple actions of secretin in the rat cerebellum. Neuroscience 134, 377–386.

Leibel, R.L., Rosenbaum, M., and Hirsch, J. (1995). Changes in Energy Expenditure Resulting from Altered Body Weight. N. Engl. J. Med. 332, 621–628.

Lerner, R.L., and Porte, D. (1970). Uniphasic insulin responses to secretin stimulation in man. J Clin Invest 49, 2276–2280.

Lerner, R.L., and Porte, D. (1972). Studies of secretin-stimulated insulin responses in man. J. Clin. Invest. 51, 2205–2210.

Li, P., Lee, K.Y., Chang, T.M., and Chey, W.Y. (1990). Mechanism of acid-induced release of secretin in rats: Presence of a secretin-releasing peptide. J. Clin. Invest. 86, 1474–1479.

Li, Y., Fromme, T., Schweizer, S., Schöttl, T., and Klingenspor, M. (2014). Taking control over intracellular fatty acid levels is essential for the analysis of thermogenic function in cultured primary brown and brite/beige adipocytes. EMBO Rep. 15, 1069–1076.

Liu, T.T. (2016). Noise contributions to the fMRI signal: An overview. Neuroimage 143, 141–151.

Lopaschuk, G.D., and Stanley, W.C. (1997). Glucose Metabolism in the Ischemic Heart. Circulation 95, 313–315.

Manabe, T., Tanaka, Y., Yamaki, K., Asano, N., Nonaka, A., Hirano, T., Nishikawa, H., and Tobe, T. (1987). The role of plasma secretin during starvation in dogs. Gastroenterol. Jpn. 22, 756–758.

Marchand, G.R. (1986). Effect of secretin on glomerular dynamics in dogs. Am. J. Physiol. 250, F256-60.

van Marken Lichtenbelt, W.D., Vanhommerig, J.W., Smulders, N.M., Drossaerts, J.M.A.F.L., Kemerink, G.J., Bouvy, N.D., Schrauwen, P., and Teule, G.J.J. (2009). Cold-activated brown adipose tissue in healthy men. N. Engl. J. Med. 360, 1500–1508.

Masci, P.G., Marinelli, M., Piacenti, M., Lorenzoni, V., Positano, V., Lombardi, M., L'Abbate, A., and Neglia, D. (2010). Myocardial structural, perfusion, and metabolic correlates of left bundle branch block mechanical derangement in patients with dilated cardiomyopathy: A tagged cardiac magnetic resonance and positron emission tomography study. Circ. Cardiovasc. Imaging 3, 482–490.

Meriläinen, P.T. (1987). Metabolic monitor. Int. J. Clin. Monit. Comput. 4, 167–177.

Metz, D.C. (2012). Diagnosis of the Zollinger-Ellison Syndrome. Clin. Gastroenterol. Hepatol. 10, 126–130.

Moolsintong, P., and Burton, F.R. (2008). Pancreatic function testing is best determined by the extended endoscopic collection technique. Pancreas 37, 418–421.

Mutt, V., Jorpes, J.E., and Magnusson, S. (1970). Structure of porcine secretin. The amino acid sequence. Eur. J. Biochem. 15, 513–519.

Mutt, V., Carlquist, M., and Tatemoto, K. (1979). Secretin-like bioactivity in extracts of porcine brain. Life Sci. 25, 1703–1707.

Ng, S.S.M., Yung, W.H., and Chow, B.K.C. (2002). Secretin as a neuropeptide. Mol. Neurobiol. 26, 97–107.

Nicholls, D.P., Riley, M., Elborn, J.S., Stanford, C.F., Shaw, C., McKillop, J.M., and Buchanan, K.D. (1992). Regulatory peptides in the plasma of patients with chronic cardiac failure at rest and during exercise. Eur. Heart J. 13, 1399–1404.

Nummenmaa, L., Hirvonen, J., Hannukainen, J.C., Immonen, H., Lindroos, M.M., Salminen, P., and Nuutila, P. (2012). Dorsal Striatum and Its Limbic Connectivity Mediate Abnormal Anticipatory Reward Processing in Obesity. PLoS One 7, e31089.

Nummenmaa, L., Saanijoki, T., Tuominen, L., Hirvonen, J., Tuulari, J.J., Nuutila, P., and Kalliokoski, K. (2018). μ-opioid receptor system mediates reward processing in humans. Nat. Commun. 9, 1500.

Nuutila, P., Koivisto, V.A., Knuuti, J., Ruotsalainen, U., Terfs, M., Haaparanta, M., Bergman, J., Solin, 0, Voipio-Pulkki, L.-M., Wegelius, U., et al. (1992). Glucose-Free Fatty Acid Cycle Operates in Human Heart and Skeletal Muscle In Vivo. J. Clin. Invest. 89, 1767–1744.

Oikonen, V. n.d. PET data analysis and modelling [WWW Document]. URL http://www.turkupetcentre.net/petanalysis/ (accessed 1.16.21).

Oikonen, V. Quantification of metabolic rate of glucose uptake with [18F]FDG.

van Ooijen, A.M.J., van Marken Lichtenbelt, W.D., van Steenhoven, A.A., and Westerterp, K.R. (2004). Seasonal changes in metabolic and temperature responses to cold air in humans. Physiol. Behav. 82, 545–553.

Orava, J., Nuutila, P., Lidell, M.E., Oikonen, V., Noponen, T., Viljanen, T., Scheinin, M., Taittonen, M., Niemi, T., Enerbäck, S., et al. (2011). Different metabolic responses of human brown adipose tissue to activation by cold and insulin. Cell Metab. 14, 272–279.

Orava, J., Nuutila, P., Noponen, T., Parkkola, R., Viljanen, T., Enerbäck, S., Rissanen, A., Pietiläinen, K.H., and Virtanen, K.A. (2013). Blunted metabolic responses to cold and insulin stimulation in brown adipose tissue of obese humans. Obesity 21, 2279–2287.

Owen, S.E., and Ivy, A.C. (1931). The Diuretic Action of Secretin Preparations. Am. J. Physiol. Content 97, 276–281.

Patlak, C.S., and Blasberg, R.G. (1985). Graphical Evaluation of Blood-to-Brain Transfer Constants from Multiple-Time Uptake Data. Generalizations. J. Cereb. Blood Flow Metab. 5, 584–590.

Paz-Filho, G., Mastronardi, C.A., and Licinio, J. (2015). Leptin treatment: Facts and expectations. Metabolism. 64, 146–156.

Peltoniemi, P., Lönnroth, P., Laine, H., Oikonen, V., Tolvanen, T., Grönroos, T., Strindberg, L., Knuuti, J., and Nuutila, P. (2000). Lumped constant for [18 F]fluorodeoxyglucose in skeletal muscles of obese and nonobese humans. Am. J. Physiol. Metab. 279, E1122–E1130.

Perry, B., and Wang, Y. (2012). Appetite regulation and weight control: The role of gut hormones. Nutr. Diabetes 2, 26.

Pissidis, A.G., Bomback, C.T., Merchant, F., and Nyhus, L.M. (1969). Hormonal regulation of bile secretion: a study in the isolated, perfused liver. Surgery 66, 1075–1084.

Polidori, D., Sanghvi, A., Seeley, R.J., and Hall, K.D. (2016). How Strongly Does Appetite Counter Weight Loss? Quantification of the Feedback Control of Human Energy Intake. Obesity 24, 2289–2295.

Ponrartana, S., Hu, H.H., and Gilsanz, V. (2013). On the relevance of brown adipose tissue in children. Ann. N. Y. Acad. Sci. 1302, 24–29.

Power, J.D., Mitra, A., Laumann, T.O., Snyder, A.Z., Schlaggar, B.L., and Petersen, S.E. (2014). Methods to detect, characterize, and remove motion artifact in resting state fMRI. Neuroimage.

Prentice, A., and Jebb, S. (2004). Energy Intake/Physical Activity Interactions in the Homeostasis of Body Weight Regulation. Nutr. Rev. 62, S98–S104.

Propst, F., Moroder, L., Wuunsch, E., and Hamprecht, B. (1979). The influence of secretin, glucagon and other peptides, of amino acids, prostaglandin endoperoxide analogues and diazepam on the level of adenosine 3',5'-cyclic monophosphate in neuroblastoma x glioma hybrid cells. J. Neurochem. 32, 1495–1500.

Pruim, R.H.R., Mennes, M., van Rooij, D., Llera, A., Buitelaar, J.K., and Beckmann, C.F. (2015). ICA-AROMA: A robust ICA-based strategy for removing motion artifacts from fMRI data. Neuroimage.

Refsum, H.E., and Strömme, S.B. (1974). Urea and creatinine production and excretion in urine during and after prolonged heavy exercise. Scand. J. Clin. Lab. Invest. 33, 247–254.

Rogers, N.H. (2015). Brown adipose tissue during puberty and with aging. Ann. Med. 47, 142–149.

Roth, G.A., Abate, D., Abate, K.H., Abay, S.M., Abbafati, C., Abbasi, N., Abbastabar, H., Abd-Allah, F., Abdela, J., Abdelalim, A., et al. (2018). Global, regional, and national age-sex-specific mortality for 282 causes of death in 195 countries and territories, 1980–2017: a systematic analysis for the Global Burden of Disease Study 2017. Lancet 392, 1736–1788.

Rothwell, N.J., and Stock, M.J. (1979). A role for brown adipose tissue in diet-induced thermogenesis. Nature 281, 31–35.

Sacks, H., and Symonds, M.E. (2013). Anatomical locations of human brown adipose tissue: Functional relevance and implications in obesity and type 2 diabetes. Diabetes 62, 1783–1790.

Saha, G.B. (2010). Basics of PET Imaging (New York, NY: Springer New York).

Saito, M., Okamatsu-Ogura, Y., Matsushita, M., Watanabe, K., Yoneshiro, T., Nio-Kobayashi, J., Iwanaga, T., Miyagawa, M., Kameya, T., Nakada, K., et al. (2009). High incidence of metabolically active brown adipose tissue in healthy adult humans: effects of cold exposure and adiposity. Diabetes 58, 1526–1531.

Sanchez-Delgado, G., Acosta, F.M., Martinez-Tellez, B., Finlayson, G., Gibbons, C., Labayen, I., Llamas-Elvira, J.M., Gil, A., Blundell, J.E., and Ruiz, J.R. (2019). Brown adipose tissue volume and 18F-fluorodeoxyglucose uptake are not associated with energy intake in young human adults. Am. J. Clin. Nutr. 00, 1–11.

Sandler, A.D., Sutton, K.A., DeWeese, J., Girardi, M.A., Sheppard, V., and Bodfish, J.W. (1999). Lack of benefit of a single dose of synthetic human secretin in the treatment of autism and pervasive developmental disorder. N. Engl. J. Med. 341, 1801–1806.

Schaffalitzky De Muckadell, O.B., and Fahrenkrug, J. (1978). Secretion pattern of secretin in man: Regulation by gastric acid. Gut 19, 812–818.

Schwarzschild, M.A., and Zigmond, R.E. (1989). Secretin and vasoactive intestinal peptide activate tyrosine hydroxylase in sympathetic nerve endings. J. Neurosci. 9, 160–166.

Schwarzschild, M.A., and Zigmond, R.E. (1991). Effects of Peptides of the Secretin-Glucagon Family and Cyclic Nucleotides on Tyrosine Hydroxylase Activity in Sympathetic Nerve Endings. J. Neurochem. 56, 400–406.

Scott, E.M., Greenwood, J.P., Vacca, G., Stoker, J.B., Gilbey, S.G., and Mary, D.A.S.G. (2002). Carbohydrate ingestion, with transient endogenous insulinaemia, produces both sympathetic activation and vasodilatation in normal humans. Clin. Sci. (Lond). 102, 523–529.

Seferovic, J.P., Claggett, B., Seidelmann, S.B., Seely, E.W., Packer, M., Zile, M.R., Rouleau, J.L., Swedberg, K., Lefkowitz, M., Shi, V.C., et al. (2017). Effect of sacubitril/valsartan versus enalapril on glycaemic control in patients with heart failure and diabetes: a post-hoc analysis from the PARADIGM-HF trial. 5, 333–340.

Sekar, R., and Chow, B.K.C. (2014). Lipolytic actions of secretin in mouse adipocytes. J. Lipid Res. 55, 190–200.

Soininen, P., Kangas, A.J., Würtz, P., Tukiainen, T., Tynkkynen, T., Laatikainen, R., Järvelin, M.-R., Kähönen, M., Lehtimäki, T., Viikari, J., et al. (2009). High-throughput serum NMR metabonomics for cost-effective holistic studies on systemic metabolism. Analyst 134, 1781.

Taubel, J., Wong, A.H., Naseem, A., Ferber, G., and Camm, A.J. (2012). Shortening of the QT interval after food can be used to demonstrate assay sensitivity in thorough QT studies. J. Clin. Pharmacol. 52, 1558–1565.

Taubel, J., Lorch, U., Ferber, G., Singh, J., Batchvarov, V.N., Savelieva, I., and Camm, A.J. (2013). Insulin at normal physiological levels does not prolong QTc interval in thorough QT studies performed in healthy volunteers. Br. J. Clin. Pharmacol. 75, 392–403.

Täubel, J., Ferber, G., Van Langenhoven, L., del Bianco, T., Fernandes, S., Djumanov, D., Kanters, J.K., Graff, C., and Camm, A.J. (2019). The Cardiovascular Effects of a Meal: J-Tpeak and Tpeak-Tend Assessment and Further Insights Into the Physiological Effects. J. Clin. Pharmacol. 59, 799–810.

Thie, J.A. (1995). Clarification of a fractional uptake concept. J. Nucl. Med. 36, 711–712.

Thörne, A., and Wahren, J. (1989). Beta-adrenergic blockade does not influence the thermogenic response to a mixed meal in man. Clin. Physiol. 9, 321–332.

Tustison, N.J., Avants, B.B., Cook, P.A., Zheng, Y., Egan, A., Yushkevich, P.A., and Gee, J.C. (2010). N4ITK: Improved N3 bias correction. IEEE Trans. Med. Imaging.

U-Din, M., Raiko, J., Saari, T., Kudomi, N., Tolvanen, T., Oikonen, V., Teuho, J., Sipilä, H.T., Savisto, N., Parkkola, R., et al. (2016). Human brown adipose tissue [15O]O2 PET imaging in the presence and absence of cold stimulus. Eur. J. Nucl. Med. Mol. Imaging.

U-Din, M., Raiko, J., Saari, T., Saunavaara, V., Kudomi, N., Solin, O., Parkkola, R., Nuutila, P., and Virtanen, K.A. (2017). Human Brown Fat Radiodensity Indicates Underlying Tissue Composition and Systemic Metabolic Health. J. Clin. Endocrinol. Metab. 102, 2258–2267.

U-Din, M., Saari, T., Raiko, J., Kudomi, N., Maurer, S.F., Lahesmaa, M., Fromme, T., Amri, E.Z., Klingenspor, M., Solin, O., et al. (2018). Postprandial Oxidative Metabolism of Human Brown Fat Indicates Thermogenesis. Cell Metab. 28, 207-216.e3.

Van der Veldt, A.A.M., Smit, E.F., and Lammertsma, A.A. (2013). Positron emission tomography as a method for measuring drug delivery to tumors in vivo: The example of [11C]docetaxel. Front. Oncol. 3 AUG.

Velmurugan, S., Brunton, P.J., Leng, G., and Russell, J.A. (2010). Circulating Secretin Activates Supraoptic Nucleus Oxytocin and Vasopressin Neurons via Noradrenergic Pathways in the Rat. Endocrinology 151, 2681–2688.

Vijgen, G.H.E.J., Bouvy, N.D., Teule, G.J.J., Brans, B., Hoeks, J., Schrauwen, P., and van Marken Lichtenbelt, W.D. (2012). Increase in Brown Adipose Tissue Activity after Weight Loss in Morbidly Obese Subjects. J. Clin. Endocrinol. Metab. 97, E1229–E1233.

Villarroya, F., Cereijo, R., Villarroya, J., and Giralt, M. (2017). Brown adipose tissue as a secretory organ. Nat. Rev. Endocrinol. 13, 26–35.

Virtanen, K.A., Peltoniemi, P., Marjamäki, P., Asola, M., Strindberg, L., Parkkola, R., Huupponen, R., Knuuti, J., Lönnroth, P., and Nuutila, P. (2001). Human adipose tissue glucose uptake determined using [18 F]-fluoro-deoxy-glucose ([18 F]FDG) and PET in combination with microdialysis. Diabetologia 44, 2171–2179.

Virtanen, K.A., Lidell, M.E., Orava, J., Heglind, M., Westergren, R., Niemi, T., Taittonen, M., Laine, J., Savisto, N.-J., Enerbäck, S., et al. (2009). Functional Brown Adipose Tissue in Healthy Adults. N. Engl. J. Med. 360, 1518–1525.

Vosselman, M.J., Brans, B., van der Lans, A.A.J.J., Wierts, R., van Baak, M.A., Mottaghy, F.M., Schrauwen, P., and van Marken Lichtenbelt, W.D. (2013). Brown adipose tissue activity after a high-calorie meal in humans. Am. J. Clin. Nutr. 98, 57–64.

Vrieze, A., Schopman, J.E., Admiraal, W.M., Soeters, M.R., Nieuwdorp, M., Verberne, H.J., and Holleman, F. (2012). Fasting and postprandial activity of brown adipose tissue in healthy men. J. Nucl. Med. 53, 1407–1410.

Waaler, B.A., Eriksen, M., and Toska, K. (1991). The effect of meal size on postprandial increase in cardiac output. Acta Physiol. Scand. 142, 33–39.

Wang, R., Chow, B.K.C., and Zhang, L. (2019). Distribution and Functional Implication of Secretin in Multiple Brain Regions. J. Mol. Neurosci. 68, 485–493.

Weir, J.B. de V. (1949). New methods for calculating metabolic rate with special reference to protein metabolism. J. Physiol. 109, 1–9.

Welle, S., Lilavivat, U., and Campbell, R.G. (1981). Thermic effect of feeding in man: increased plasma norepinephrine levels following glucose but not protein or fat consumption. Metabolism. 30, 953–958.

WH, Y., PS, L., SS, N., J, Z., SC, C., and BK, C. (2001). Secretin Facilitates GABA Transmission in the Cerebellum. J. Neurosci. 21.

Wilson, J.R., Reichek, N., Dunkman, W.B., and Goldberg, S. (1981). Effect of diuresis on the performance of the failing left ventricle in man. Am. J. Med. 70, 234–239.

Yamagata, T., Urano, H., Weeber, E.J., Nelson, D.L., and Nishijima, I. (2008). Impaired hippocampal synaptic function in secretin deficient mice. Neuroscience 154, 1417–1422.

Yang, Y., and Zhang, J. (2020). Bile acid metabolism and circadian rhythms. Am. J. Physiol. - Gastrointest. Liver Physiol. 319, G549–G563.

Yang, H., Wang, L., Wu, S. V., Tay, J., Goulet, M., Boismenu, R., Czimmer, J., Wang, Y., Wu, S., Ao, Y., et al. (2004). Peripheral secretin-induced Fos expression in the rat brain is largely vagal dependent. Neuroscience 128, 131–141.

Yoneshiro, T., Aita, S., Matsushita, M., Kayahara, T., Kameya, T., Kawai, Y., Iwanaga, T., and Saito, M. (2013). Recruited brown adipose tissue as an antiobesity agent in humans. 123, 3404–3408.

Young, L.J. (2001). Oxytocin and vasopressin as candidate genes for psychiatric disorders: lessons from animal models. AM J Med Genet 105, 53–54.

Zhang, Y., Brady, M., and Smith, S. (2001). Segmentation of brain MR images through a hidden Markov random field model and the expectation-maximization algorithm. IEEE Trans. Med. Imaging.

Zwillich, C., Martin, B., Hofeldt, F., Charles, A., Subryan, V., and Burman, K. (1981). Lack of effects of beta sympathetic blockade on the metabolic and respiratory responses to carbohydrate feeding. Metabolism 30, 451–456.

TURUN
YLIOPISTO
UNIVERSITY
OF TURKU